REPORT No. 188
GEOLOGICAL SURVEY OF JAPAN

# ON THE DISTRIBUTION OF GAMMA RAY INTENSITY DUE TO NATURAL RADIOACTIVITY NEAR THE EARTH'S SURFACE

By
Shun-ichi SANO

GEOLOGICAL SURVEY OF JAPAN
Hisamoto-chō, Kawasaki-shi, Japan
1961

539.166:550.35

**REPORT No. 188**

GEOLOGICAL SURVEY OF JAPAN

Katsu KANEKO, Director

# On the Distribution of Gamma Ray Intensity due to Natural Radioactivity near the Earth's Surface

By

Shun-ichi SANO

# CONTENTS

# On the Distribution of Gamma Ray Intensity due to Natural Radioactivity near the Earth's Surface

By

Shun-ichi SANO

**Abstract**

Among the several investigations on the distribution of gamma ray intensity due to terrestrial radioactivity, the principle developed by A. Y. Sakakura is considered to be the most reasonable. The use of the linear build up factor is, however, more suitable so far as the usual measurement of the terrestrial radioactivity is concerned. Therefore, the inverse-square exponential law for a point isotropic source combined with a linear build up factor was applied to the calculation of gamma ray intensity in the air and in a drill hole.

The measurement of gamma ray intensity in the air from a broad source or an effective half-space was made at various altitudes over a sand area on the coast of the Sea of Japan. The values of a scattering constant for air composed of a build up factor were determined for the detector currently used so as to fit the above experimental data by assuming several values of absorption coefficient. A reasonable value of scattering constant was obtained in the case of the absorption coefficient of $4.5\times10^{-5}\,\mathrm{cm}^{-1}$ for the most penetrating ray from natural radioactive substances. Simple inverse-square exponential law is also applicable to the calculations of gamma ray intensity in the air by assuming the smaller value of $3.5\times10^{-5}\mathrm{cm}^{-1}$ for the absorption coefficient of air. The gamma ray intensities directly over an elementary slab source at various altitudes were calculated by using the constants thus obtained, and the results were consistent with the experimental data by a similar detector.

The fundamental formula for a point source was transformed to the expression for an elementary source of infinite thickness. This expression is useful for many problems concerning the intensity distribution in air. The infinitely thick source is represented by the areal distribution on the ground surface. The dimensions of sources equivalent to the broad source were estimated in the case of circular and infinite slab sources, and the results were in agreement with the calculations, which were made by utilizing the different mathematical expressions and the analogous experimental data. The intensity distributions over the boundary of two effective broad sources were also calculated.

The intensity distributions from a small thick source and an infinite slab source were calculated, as the representatives of infinitely thick sources, in order to supply knowledge on the intensity distributions at various altitudes. The characteristics of distributions, namely, the width at half-maximum intensity and the maximum intensity normalized to the broad source intensity at an altitude of 200 m, were illustrated in the form of charts convenient for the analysis of the airborne survey data.

The variations in gradient of the intensity-altitude curve plotted on the semi-log graph were discussed in order to understand the causes of errors in the altitude correction, which is usually followed by the broad source curve. Excluding clearly exceptional cases, we discussed three possible causes. The most important cause may be the topographic effect, in which the gradients of curve are nearly equal to those of a broad

source curve over a definite position of topographic section, but whose apparent variations in gradients depend upon the relative directions between flight line and topography. Another cause to be considered is the effect of such a surface layer, as the weathering layer or the artificial radioactive substances, which are absorbed in the ground surface, and the indirect effect caused by airborne radioactive substances. Investigations into the latter two effects have never been done sufficiently, because of the lack of knowledge which has prevented us from directly comparing the effects with the airborne survey data.

The intensity distributions in a bare drill hole from a horizontal radioactive layer were calculated by substituting a line detector for an actual one. The substitution is considered to be a proper assumption for the discussion concerning the effects of detector length and hole diameter in the response of the detector. The effects intuitionally expected were theoretically shown in the figures, which represent the relationships between the characteristics of intensity distribution and the thickness of the radioactive layer. The figures show examples of charts estimating the grade and the thickness of ore bearing layer from a radioactivity log.

The values of the constant composing the build up factor were determined for the actual detectors by the experimental intensity distributions from the artificial ore bearing layers, while the results were affected by the difference in directional character between the theoretical and the actual detector. The theoretical expression is, however, still useful as an approximation for the intensity distribution.

The products of the grade and the thickness of the horizontal ore bearing bed, which are necessary for an estimation of the ore reserves, are obtained by integrating the intensity in the drill hole with respect to its depth, but independent of the hole diameter as well as of the dynamic character of the ratemeter.

In the Appendix, the examples of estimation of gamma ray intensity on the ground surface were set forth by applying the fundamental formula for an elementary source of infinite thickness. It is notable that the gamme ray intensity from the infinite slab source is proportional to the minimum angle between the two planes, which contain the detector and the boundary of the source.

## I. Introduction

The distribution of gamma ray intensity can be calculated by tracing the behavior of photons through the medium, as the interactions of gamma ray with matter are well known. For this purpose several methods have been proposed and have been mainly applied to the field of the designing shield of the atomic reactor. On the other hand, the intensity distribution can be determined by assuming a law of attenuation as the function of distance for an elementary source, and the intensity distributions can be calculated by integrating the law over the geometric configuration of sources. With respect to the law, the inverse-square exponential law for a point source is well known and has been widely used. For instance, E. Rothè[8], using this law, discussed the measurement of gamma ray intensity on the ground due to natural radioactivity near the earth's surface, that is, terrestrial radioactivity. However, deviations from this law due to the scattering component of radiation must be taken into consideration and the so-called build up factor, which corrects the deviation from the inverse-square exponential law, must be obtained.

J. C. Cook[3] calculated the distributions of gamma ray intensity in the

air based on a law containing the effect of scattering. The law of attenuation was expressed as an empirical formula fitting the computed intensity variation for an effective energy of natural gamma radiation based on the experiments by a point source immersed in a large medium. A. Y. Sakakura[9] pointed out that "there is no priori reason why any effective quantity computed or measured in one source to medium orientation should be applicable to others." Therefore, he considered an elementary source of infinite thickness, under the consideration of the ground depth, in order to analyse quantitatively the anomalous gamma ray intensity discovered by airborne surveys. He used the law of attenuation expressed as a polynominal equation with respect to distance, which was proposed by U. Fano[5]. But, his expression for the law is reduced formally to a formula for a point source, while the build up factor is nothing but a polynominal equation of second order, the linear term of which has a definite value.

The present paper gives the law of attenuation for a point source expressed by the inverse-square exponential law combined with the linear build up factor, because, in the writer's opinion, the square term is unnecessary as far as the usual measurement of gamma ray intensity due to terrestrial radioactivity is concerned. The constant for air composing the build up factor and the constants concerned with the properties of the source substance and the detector are determined following the procedure developed by Sakakura[9].

Since the present law of attenuation is applied to a point source, the discussions on the intensity distributions are extended to those distributions from sources of finite thickness. The constant for the terrestrial medium is estimated from the experiments in a drill hole containing artificial radioactive layers, although an accurate evaluation is difficult to be obtained by the effects of the shape and the dimension of the detector.

The measurements of distribution of gamma ray intensity due to terrestrial radioactivity are practically applied in prospecting for uranium ores. The main purpose of these surveys consists in limiting the areas where geological and mineralogical studies will be carried out. Surface distributions of radioactive substances do not faithfully represent underground deposits, but are only information or indications of deposits. Therefore, quantitative analysis of distributions is not requisite. On the other hand, quantitative analysis is desirable for the measurement in the drill holes or in the adit of mines, because fresh deposits can be seen in these openings. Complete quantitative analysis is, however, obstructed by the presence of substances of various types of disequilibrium in the uranium series and the presence of substances containing both the uranium and the thorium series. Thus, the most interesting and important matter is thought to be in finding some typical features of gamma ray intensity distribution from several source types.

The measurement of the radioactivity of rocks and of the anomalous intensity from exposures of deposit should be made carefully, since the content of radioactive substances in ordinary rock sometimes has a relationship to various kinds of deposits. Therefore, it is important to make the altitude correction for the intensity from a source extended in a semi-infinite medium. Thus the relationships between the intensity in the air and the altitude from the terrain are mainly discussed here for extensive sources which are along

the ground surface, since the variation in the intensity-altitude relationship might yield considerable errors in correcting the intensities at various altitudes to those at a certain altitude. The intensity distributions in the air from several typical sources already have been discussed in detail by Sakakura[9], but his investigation was limited to the altitude of 500 feet. The present writer discusses the intensity distributions from two extreme types of source at various altitudes.

Moreover, this paper deals with the measurement in a drill hole or a natural gamma ray logging in the case of the horizontal layer by using a line detector.

**Acknowledgments**

The writer wishes to express his sincere thanks to Dr. Kumiji Iida, Professor of Nagoya University, for his kind guidance and advice. Cordial thanks are also due to Dr. Naomo Miyabe for his valuable discussions.

## II. Law of Gamma Ray Attenuation

### II. 1 Description of Law and Fundamental Formula

The law of attenuation described here is frequently used in a designing shield for radiation from a radioisotope[1].

Suppose a point radiation detector and an elementary volume emitting isotropically gamma rays in a space, which is filled with various media, as shown in Fig. 1. The following symbols are used:

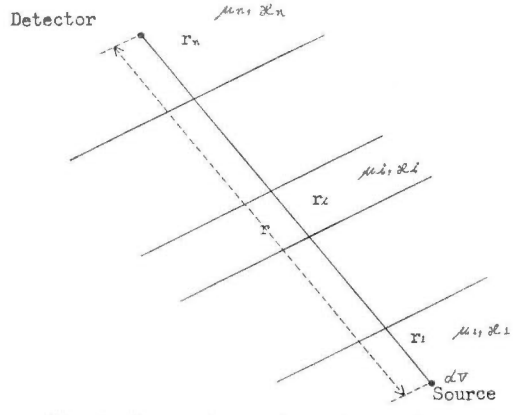


Fig. 1 Source in an elementary volume

$I$: gamma ray intensity measured by detector
$I_0$: constant depending upon the property of source substance and the sensitivity of detector
$\sigma$: content of radioactive source
$r$: distance between detector and center of source
$r_i$: length of straight line connecting detector and source in a medium

$\mu_i$: linear absorption coefficient of a medium
$\kappa_i$: scattering constant of a medium
$n$: number of medium through which the straight line from source to detector passes
$dV$: elementary volume

The fundamental formula is expressed by

$$I=I_0\sigma\left(\frac{e^{-\sum_{i=1}^{n}\mu_i r_i}}{4\pi r^2}+\sum_{i=1}^{n}\kappa_i\mu_i r_i\,\frac{e^{-\sum_{i=1}^{n}\mu_i r_i}}{4\pi r^2}\right)dV=I_0\sigma\left(1+\sum_{i=1}^{n}\kappa_i\mu_i r_i\right)\frac{e^{-\sum_{i=1}^{n}\mu_i r_i}}{4\pi r^2}\,dV, \qquad (1)$$

where, $I_0\sigma e^{-\sum_{i=1}^{n}\mu_i r_i}/4\pi r^2$ is called the absorption term and $I_0\sigma\sum_{i=1}^{n}\kappa_i\mu_i r_i\cdot e^{-\sum_{i=1}^{n}\mu_i r_i}/4\pi r^2$ is called the scattering term. The factor, $1+\sum_{i=1}^{n}\kappa_i\mu_i r_i$, is the build up factor.

Energy spectra of gamma rays emitted from uranium series and thorium series which are important natural radioactive elements are quite complex, whereas the absorption coefficient and scattering constant are assumed to be independent of energy spectrum. After gamma rays penetrate through the medium down to a moderate depth, gamma ray intensity is governed by scattered rays, whose energy level is nearly equal to that of the most penetrating ray[5]. Thus, the absorption coefficient in the fundamental formula (1) should have the value corresponding to the most penetrating gamma ray, while scattering term should contain the effects of primary gamma rays of low penetrating power, as well as secondary gamma rays.

Uranium and thorium series are both important natural radioactive elements. Rocks and minerals sometime contain uranium series together with thorium series at various ratios. Integral energy spectra of both series are rather similar to each other, but different from those of artificial radioactive elements. Uranium series contained in ores are frequently in disequilibrium, but the majority of gamma rays from uranium series are radiated from daughters of $^{222}$Rn, while the energy spectrum is not much affected by disequilibrium. The most penetrating rays for various media are about 2.4MeV ray with the uranium series and about 2.6 MeV ray with the thorium series; the absorption coefficient for these gamma rays are practically equal to each other. Therefore, the scattering constant also is considered to be independent of the uranium-thorium ratio or disequilibrium of the uranium series. The contents $\sigma$ is called as grade and often is expressed by the equivalent uranium content eU. Then, the constant $I_0$ varies with the uranium-thorium ratio or disequilibrium of the uranium series. The scattering constant $\kappa_i$ depends upon the energy response of the detector, except when intensity is measured in dose rate.

The detector is considered as a point, except when it is close to the source. If the detector has a directional character that depends only upon angles around it, the constant $I_0$ contains functions of angles which represent directional character.

### II. 2 Co-ordinate System

In order to calculate the distribution of gamma ray intensity, the fundamental formula (1) is integrated over source geometry. A co-ordinate system $(Z, \theta, \varphi)$, which may be called a conic co-ordinate system, is a kind of curvilinear

co-ordinate system, and is useful when the surface of source is a plane. The relationships to the rectangular co-ordinate system $(x, y, z)$ are given by

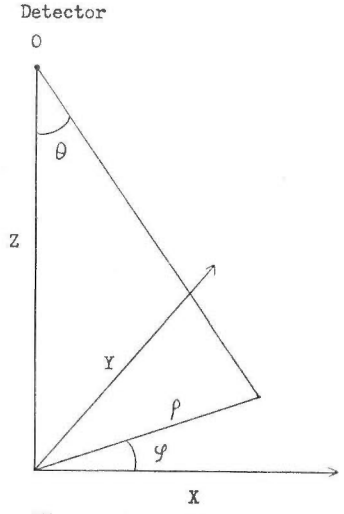


Fig. 2 Co-ordinate system

$$x=Z\tan\theta\cos\varphi, \qquad y=Z\tan\theta, \qquad z=Z, \tag{2}$$

where the origins and $z$ axis are common, as shown in Fig. 2. The volume element, therefore, is expressed as

$$dV=dxdydz=Z^2\tan\theta\sec^2\theta\, dZ\, d\theta d\varphi=Z^2\sec\theta\, dZd(\sec\theta)\, d\varphi. \tag{3}$$

In this paper, the origin of the co-ordinate system $(Z, \theta, \varphi)$ is always located at the conter of the detector, and the $Z$ axis is always perpendicular to the surface of source.

The fundamental formula (1) is rewritten as

$$I=\frac{I_0\sigma}{4\pi}(1+\sum_{i=1}^{n}\kappa_i\mu_i Z_i\sec\theta)\frac{e^{-\sum_{i=1}^{n}\mu_i Z_i\sec\theta}}{\sec\theta}dZd(\sec\theta)d\varphi=I'dZd(\sec\theta)d\varphi,$$

where $r_i=Z_i\sec\theta$, as long as the boundaries of media are perpendicular to the $Z$ axis.

The integration with respect to $Z$ is always possible. If $\theta$ and $\varphi$ are independent of $Z$ and the detector is non-directional or has directional character represented by $\cos^n\theta$, distributions of gamma ray intensity can be given by exponential integrals or integrals containing exponential integrals. The exponential integrals are of the form of

$$En(x)=\int_x^\infty\frac{e^{-\zeta}}{\zeta^n}d\zeta, \tag{4}$$

and several numerical tables already have been published. If the detector has a directional character represented by $\sin^n\theta$, the distributions of gamma ray intensity are given in similar form with the integrals

$$E'_{m,n}(x) = \int_{\zeta=x}^{\zeta=\infty} \sqrt{(\alpha^2\zeta^2-\alpha^2)^m/(\alpha\zeta)^n} \cdot e^{-\alpha\zeta}\, d(\alpha\zeta). \qquad (5)$$

These integrals have never been calculated, since the detector of such directional character is less sensitive, and is rarely put to practical use.

## III. Attenuation in Air

### III. 1 Fundamental Sources and Experiments

Attenuation of gamma rays due to terrestrial radioactivity in air is an important element in airborne radiometric surveyings, although this element is usually negligible in measurements of the ground or in a drill hole. For example, the altitude correction for gamma ray intensity in air is required if flight levels can not be kept constant from the terrain.

The constants for air in the fundamental formula are obtained by experiments following the method developed by A. Y. Sakakura[9]. He selected two types of source for the fundamental sources and determined the constants in his expression by using experimental data over these sources. The one, a broad source, is a half-space filled homogeneously with radioactive substances and the other, an elementary slab source, is a semi-infinite vertical pillar embedded in the ground. For the determination of constants, however, two types are excessive.

The actual broad source[9], over which the measurements of gamma ray intensity were made from 100 to 1000 feet above the ground, was an area of Mancos shale of several square miles. Representative trench samples of the shale contained 1.6 % K, 0.0017 % U, and 0.0013 % equivalent U. The actual elementary slab source[9] was a slab of 40 feet square and 6 inches thick and contained 48 tons of carnotite ore at 0.35 % $U_3O_8$, as shown in Fig. 3. The measurements over the source were made from 100 to 550 feet above the ground, but the effect of dynamic character of ratemeter was noticed at altitudes less than 450 feet.

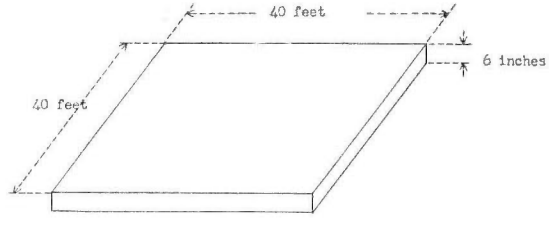


Fig. 3 Actual elementary slab source
(U. S. Atomic Energy Commission)

We carried out the measurements over a broad source, which is an area of sand near Niigata city, on the coast of the Sea of Japan. The range of altitudes was extended up to 500 m. The sand probably contains a considerable amount of thorium, but the relationship between the gamma ray intensity and the altitude shows fair agreement with that obtained over the Mancos

shale area. Scintillation detectors used in our experiments consist of a 5 inch photomultiplier and a sodium iodide crystal 5 inches in diameter and 2 inches thick. Output signals from two detectors were mixed to feed the ratemeter. The directional character was examined by repeating flights with different arrangements of detectors, and it was proved that detectors are non-directional.

In order to obtain the contribution due to the broad source or to obtain the terrestrial radioactivity from counting rates measured by the detector, the counting rate above the sea was subtracted from gross counting rates. The counting rate above the sea, which is called zero background, was unchanged in the period of the measurements and independent of altitudes or distances from the sea shore. The results of the experiment are shown in Sec. III.4.

### III. 2 Integrals for the Broad Source

In evaluating the integrals over a broad source, the following symbols are necessary in addition to those referred to in Chap. II.

$I^B$: gamma ray intensity from a broad source
$\mu_a$: linear absorption coefficient of air
$\mu_1$: linear absorption coefficient of source media, that is, self absorption coefficient
$\kappa_a$: scattering constant of air
$\kappa_1$: scattering constant of source media
$Z_0$: altitude of detector

Although the detector used in the experiment is non-directional, we considered several directional detectors for reference.

(1) Directional character is such that $I_0$ is replaced by $I_0 \cos^n\theta$.

$$I^B=\int_{Z_0}^{\infty}\int_1^{\infty}\int_0^{2\pi} I'\cos^n\theta\, dZd(\sec\theta)d\varphi$$
$$=(1+\kappa_1)\frac{I_0\sigma}{2\mu_1}(\mu_a Z_0)^{n+1}E_{n+2}(\mu_a Z_0)+\kappa_a\frac{I_0\sigma}{2\mu_1}(\mu_a Z_0)^{n+1}E_{n+1}(\mu_a Z_0)\,, \qquad (6)$$

when the detector is non-directional, $n=0$ and we have

$$I^B=(1+\kappa_1)\frac{I_0\sigma}{2\mu_1}(\mu_a Z_0)E_2(\mu_a Z_0)+\kappa_a\frac{I_0\sigma}{2\mu_1}(\mu_a Z_0)E_1(\mu_a Z_0). \qquad (7)$$

(2) Directional character is such that $I_0$ is replaced by $I_0\sin^n\theta$.

$$I^B=\int_{Z_0}^{\infty}\int_1^{\infty}\int_0^{2\pi} I'\sin^n\theta dZ\, d(\sec\theta)d\varphi$$
$$=(1+\kappa_1)\frac{I_0\sigma}{2\mu_1}(\mu_a Z_0)E'_{n,\,n+2}(\mu_a Z_0,\,1)+\kappa_2\frac{I_0\sigma}{2\mu_1}E'_{n,\,n+1}(\mu_a Z_0,\,1)\,. \qquad (8)$$

(3) Directional character is such that $I_0$ is constant for $[0\leqq\theta\leqq\theta_0,\ (2\pi-\theta_0)\leqq\theta\leqq 2\pi]$ and zero for $[\theta_0<\theta<(2\pi-\theta_0)]$.

This character is realized approximately by shielding the side of the detector.

$$I^B=\int_{Z_0}^{\infty}\int_1^{\sec\theta_0}\int_0^{2\pi} I'dZd(\sec\theta)d\varphi$$

$$=(1+\kappa_1)\frac{I_0\sigma}{2\mu_1}(\mu_a Z_0)\{E_2(\mu_a Z_0)-E_2(\mu_a Z_0 \sec\theta)\}$$
$$+\kappa_a\frac{I_0\sigma}{2\mu_1}(\mu_a Z_0)\{E_1(\mu_a Z_0)-E_1(\mu_a Z_0 \sec\theta_0)\} \qquad (9)$$

(4) Directional character is such that $I_0$ is replaced by $I_0 \frac{\cos^n}{\sin^n}\varphi$.

In this case, Eq. (7) is multiplied by $4\int_0^{\pi/2} \frac{\cos^n}{\sin^n}\varphi d\varphi$.

As seen in the formulae, the self absorption coefficient $\mu_1$ appears only in the denominator of the constant factors. Therefore, an increase in $\mu_1$ is equivalent to a decrease in $\sigma$. The matter is quite similar with the terms containing a scattering constant of source medium.

### III. 3 Integrals for Elementary Slab Source

Gamma ray intensity from a slab source, as shown in Fig. 3, is easily obtained if the slab is replaced by the base of a square cone, whose apex is a detector and whose generating lines go through the sides of the upper surface. When the altitude of the detector is very high compared with the dimensions of the slab, the replacement is a good approximation, since the deviation of actual form of the source is disregarded.

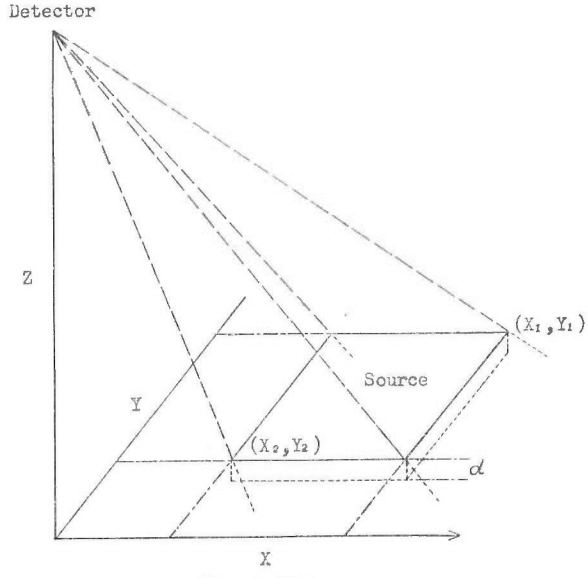


Fig. 4 Slab source

A rectangular co-ordinate system $(x, y)$ is taken on the groud surface, which coincides with the upper surface of the source, and the origin lies on the $Z$ axis of the conic co-ordinate system $(Z, \theta, \varphi)$, as shown in Fig. 4. The sides of the slab surface are parallel to the $x$ or $y$ axis, while the co-ordinate of the two opposite apexes of the rectangle are $(x_1, y_1)$ and $(x_2, y_2)$. Then, the gamma ray intensity by the slab $I^S$ is

$$I^S(x_1, y_1 : x_2, y_2) = I^S(x_1, y_1 : 0, 0) + I^S(x_2, y_2 : 0, 0) \mp I^S(x_2, y_1 : 0, 0) \mp I^S(x_1, y_2 : 0, 0) \tag{10}$$

When the detector is non-directional, the integral $I^S$ is given by

$$\begin{aligned}
I^S(x, y : 0, 0) &= \int_{Z_0}^{\infty}\int_{1}^{\frac{\sqrt{x^2\sec^2\varphi + Z_0^2}}{Z_0}}\int_{0}^{\tan^{-1}|y/x|} I' dZ d(\sec\theta) d\varphi \\
&\quad + \int_{Z_0}^{\infty}\int_{1}^{\frac{\sqrt{Z_0^2 + y^2\,\mathrm{cosec}^2\varphi}}{Z_0}}\int_{\tan^{-1}|y/x|}^{\pi/2} I' dZ d(\sec\theta) d\varphi \\
&= (1+\kappa_1)\frac{I_0\sigma}{8\mu_1}\left[(\mu_a Z_0)E_2(\mu_a Z_0) - (\mu_a Z_0 + \mu_1 d)E_2(\mu_a Z_0 + \mu_1 d)\right] \\
&\quad + \frac{I_0\sigma}{8\mu_1}\left[\kappa_a(\mu_a Z_0)E_1(\mu_a Z_0) - (\kappa_a\mu_a Z_0 + \kappa_1\mu_1 d)(\mu_a Z_0 + \mu_1 d)E_1(\mu_a Z_0 + \mu_1 d)\right] \\
&\quad - (1+\kappa_1)\frac{I_0\sigma}{4\pi\mu_1}\left\{\int_0^{\tan^{-1}|y/x|}\left[(\mu_a Z_0)E_2(\mu_a\sqrt{Z_0^2 + x^2\sec^2\varphi}\right.\right. \\
&\quad \left.\left. - (\mu_a Z_0 + \mu_1 d)E_2\left\{(\mu_a Z_0 + \mu_1 d)\frac{\sqrt{Z_0^2 + x^2\sec^2\varphi}}{Z_0}\right\}\right]d\varphi\right. \\
&\quad \left. + \int_{\tan^{-1}|y/x|}^{\pi/2}\left[(\mu_a Z_0)E_2(\mu_a\sqrt{Z_0^2 + y^2\,\mathrm{cosec}^2\varphi}\right.\right. \\
&\quad \left.\left. - (\mu_a Z_0 + \mu_1 d)E_2\left\{(\mu_a Z_0 + \mu_1 d)\frac{\sqrt{Z_0^2 + y^2\,\mathrm{cosec}^2\varphi}}{Z_0}\right\}\right]d\varphi\right\} \\
&\quad - \frac{I_0\sigma}{4\pi\mu_1}\left\{\int_0^{\tan^{-1}|y/x|}\left[\kappa_a(\mu_a Z_0)E_1(\mu_a\sqrt{Z_0^2 + x^2\sec^2\varphi})\right.\right. \\
&\quad \left.\left. - (\kappa_a\mu_a Z_0 + \kappa_1\mu_1 d)(\mu_a Z_0 + \mu_1 d)E_1\left\{(\mu_a Z_0 + \mu_1 d)\frac{\sqrt{Z_0^2 + x^2\sec^2\varphi}}{Z_0}\right\}\right]d\varphi\right. \\
&\quad \left. + \int_{\tan^{-1}|y/x|}^{\pi/2}\left[\kappa_a(\mu_a Z_0)E_1(\mu_a\sqrt{Z_0^2 + y^2\,\mathrm{cosec}^2\varphi})\right.\right. \\
&\quad \left.\left. - (\kappa_a\mu_a Z_0 + \kappa_1\mu_1 d)(\mu_a Z_0 + \mu_1 d)E_1\left\{(\mu_a Z_0 + \mu_1 d)\frac{\sqrt{Z_0^2 + y^2\,\mathrm{cosec}^2\varphi}}{Z_0}\right\}\right]d\varphi\right\}.
\end{aligned} \tag{11}$$

When the detector is located above the center of the source, whose surface is square, and $d$ is infinitely large, the above integral is simplified as

$$\begin{aligned}
I^S &= (1+\kappa_1)\frac{I_0\sigma}{2\mu_1}\left[(\mu_a Z_0)E_2(\mu_a Z_0) - \frac{4}{\pi}\int_0^{\pi/2}\{(\mu_a Z_0)E_2(\mu_a\sqrt{Z_0^2 + A^2\sec^2\varphi})\}d\varphi\right] \\
&\quad + \kappa_a\frac{I_0\sigma}{2\mu_1}\left[(\mu_a Z_0)E_1(\mu_a Z_0) - \frac{4}{\pi}\int_0^{\pi/2}(\mu_a Z_0)E_1(\mu_a\sqrt{Z_0^2 + A^2\sec^2\varphi})d\varphi\right],
\end{aligned} \tag{12}$$

where $2A$ is taken for the length of the side of the square source.

In Eq. (12), the self absorption coefficient $\mu_1$ appears in the denominator of the constant factor, just like the formulae for the broad source. This result is valid for any source types of infinite thickness.

### III. 4 Determination of Constants

The constant factors in the expressions for gamma ray intensity from the fundamental sources of infinite thickness are $I_0\sigma(1+\kappa_1)/(2\mu_1)$ and $I_0\sigma\kappa_a/(2\mu_1)$. These values should be determined so as to fit the experimental relationship between gamma ray intensity and altitude over the fundamental sources, if the proper value of $\mu_a$ is given.

The constants of source medium, $\mu_1$ and $\kappa_1$, was determined from experiments by other kinds of source on the ground and then $\kappa_a$ was determined. However, $\mu_1$ and $\kappa_1$ are rather invariable compared with the variation of $\sigma$. As for the estimation of gamma ray intensity, the calculation of the values of two constant factors are enough for sources which are infinitely thick and have a plane surface.

The values of $I_0\sigma(1+\kappa_1)/(2\mu_1)$ and $I_0\sigma\kappa_a/(2\mu_1)$ were calculated by means of least square from our broad source data over the sand area near Niigata city. The values of ratio, $\kappa_a/(1+\kappa_1)$ are given in Table 1 and calculated intensity-altitude relationships are shown in Fig. 5 with experimental data.

Table 1

| $\mu_a$ (cm$^{-1}$) | $\kappa_a/(1+\kappa_1)$ | $\sigma$ (% eU) of Mancos shale |
|---|---|---|
| $3.5\times10^{-5}$ | 0.00 | 0.0015 |
| $4.5\times10^{-5}$ | 0.307 | 0.0015 |
| $5.9\times10^{-5}$ | 0.987 | 0.0014 |

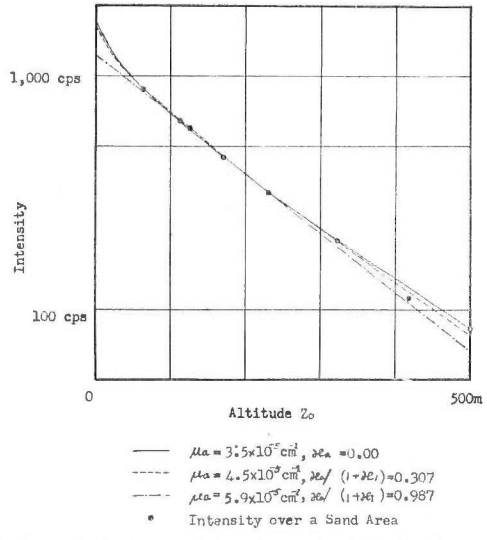


Fig. 5 Relationship between intensity and altitude for a broad source

The value of $\mu_a$ used by A. Y. Sakakura[9] is $4.5\times10^{-5}$ cm$^{-1}$, which corresponds to the absorption coefficient for the most penetrating ray of uranium series. In addition to this value, our calculations were made by using the other two values. The one, $3.5\times10^{-5}$ cm$^{-1}$, is the "true" absorption coefficient in the effective energy range of gamma rays from the uranium or thorium series. The other, $5.9\times10^{-5}$ cm$^{-1}$, used after J. C. Cook[3], corresponds to the absorption coefficient of 1.8 MeV gamma ray. As for the intensity-altitude relationships, the curves for $\mu_a=3.5\times10^{-5}$ cm$^{-1}$ and $\mu_a=4.5\times10^{-5}$ cm$^{-1}$ almost coincide with each other, and the curve for $\mu_a=5.9\times10^{-5}$ cm$^{-1}$ shows a deviation from the other curves and experimental data.

The intensity-altitude relationship directly over the actual elementary slab source was calculated by Eq. (12) by utilizing the values of $\kappa_a/(1+\kappa_1)$ obtained above. We checked the assumption of $d=\infty$ in Eq. (12) through Eq. (11) when $\mu_1=0.2\,\mathrm{cm}^{-1}$ and $\kappa_1=1$ and found out that the actual source is equivalent to a semi-infinite pillar embedded in the ground. The factor $I_0\sigma/(2\mu_1)$ was adjusted so as to fit the measured intensity at altitudes from 450 to 600 feet. The calculated intensity-altitude relationships and experimental data are shown in Fig. 6. Deviations of the curves from the experimental data* at altitudes less than 450 feet can be explained by introducing the effect of dynamic character of ratemeter[9]. We obtained the value of $(1+\kappa_1)I_0/(2\mu_1)$ for the detector used in these experiments, since $\sigma$ of the elementary slab source was known, and then calculated the grade of Mancos shale from experimental data over the source. The results are shown in Table 1 which agree well with the uranium contents of the samples.

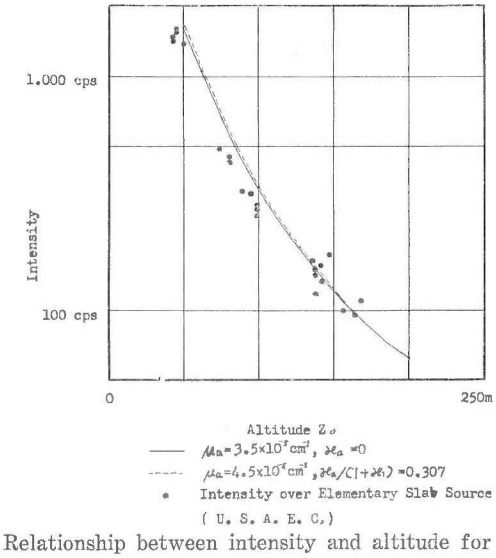


Fig. 6 Relationship between intensity and altitude for the actual elementary slab source

By the way, the value of $(1+\kappa_1)I_0/(2\mu_1)$ for the airborne instrument which is currently used by the Geological Survey of Japan is estimated to be about $2\times10^6$ cps/percent eU.

So far as the present phenomenological theory is concerned, it is convenient to adopt the values of $3.5\times10^{-5}\,\mathrm{cm}^{-1}$ for $\mu_a$ and zero for $\kappa_a$ for the sake of simplicity of calculations.

### III. 5 Effect of Surface Layer

In this section intensity-altitude relationship are considered when the half-space is composed of layers. A half-space is separated into several horizontal layers, as shown in Fig. 7 and radioactive substances are contained homogeneously in each layer. The additional symbols for this case are explained as follows:

* These experimental data are also referred to in "Nuclear Geology" 1954, John Wiley & Sons. Inc. (U. S. A.) p. 228~229

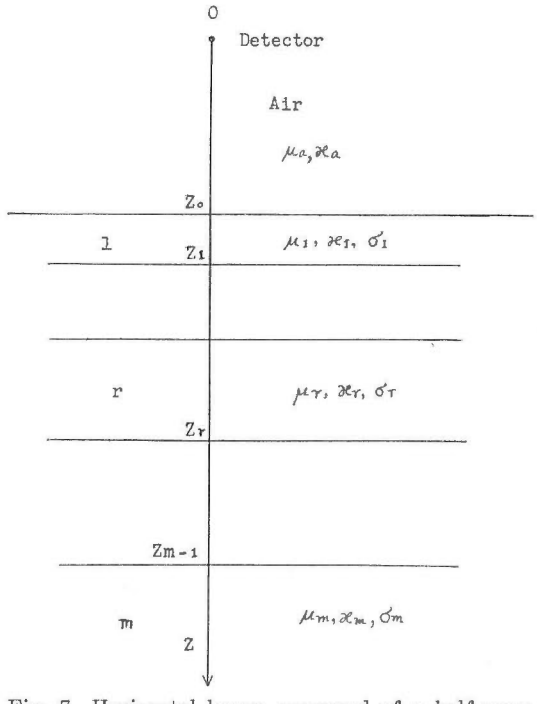


Fig. 7 Horizontal layers composed of a half-space

$I^{B'}$: gamma ray intensity from a layered half-space
$\sigma_r$: grade of $r$th layer
$\mu_r$: linear absorption coefficient of $r$th layer
$\kappa_r$: scattering constant of $r$th layer
$Z_r$: height of detector from lower boundary of $r$th layer
$m$: number of layer

The thickness of the $m$th layer is infinitely thick. Then,

$$
\begin{aligned}
I^{B'} &= \int_{Z_0}^{\infty}\int_{1}^{\infty}\int_{0}^{2\pi} I' dZ d(\sec\theta) d\varphi \\
&= (1+\kappa_1)\frac{I_0\sigma_1}{2\mu_1}(\mu_a Z_0)E_2(\mu_a Z_0)+\kappa_a\frac{I_0\sigma_1}{2\mu_1}(\mu_a Z_0)E_1(\mu_a Z_0) \\
&+\frac{I_0}{2}\sum_{r=2}^{m}\left(\frac{\sigma_r}{\mu_r}-\frac{\sigma_{r-1}}{\mu_{r-1}}\right)\{\mu_a Z_0+\sum_{i=1}^{r-1}\mu_i(Z_i-Z_{i-1})\}E_2\{\mu_a Z_0+\sum_{i=1}^{r-1}\mu_i(Z_i-Z_{i-1})\} \\
&+\frac{I_0}{2}\sum_{r=2}^{m}\left(\frac{\kappa_r\sigma_r}{\mu_r}-\frac{\kappa_{r-1}\sigma_{r-1}}{\mu_{r-1}}\right)\{\mu_a Z_0+\sum_{i=1}^{r-1}\mu_i(Z_i-Z_{i-1})\}E_2\{\mu_a Z_0+\sum_{i=1}^{r-1}\mu_i(Z_i-Z_{i-1})\} \\
&+\frac{I_0}{2}\sum_{r=2}^{m}\left(\frac{\sigma_r}{\mu_r}-\frac{\sigma_{r-1}}{\mu_{r-1}}\right)\{\kappa_a\mu_a+\sum_{i=1}^{r-1}\kappa_i\mu_i(Z_i-Z_{i-1})\}\{\mu_a Z_0+\sum_{i=1}^{r-1}\mu_i(Z_i-Z_{i-1})\} \\
&\times E_1\{\mu_a Z_0+\sum_{i=1}^{r-1}\mu_i(Z_i-Z_{i-1})\}. \qquad (13)
\end{aligned}
$$

If there is one surface layer or $m=2$, and the thickness of the surface layer is $d$,

$$
I^{B'}=(1+\kappa_1)\frac{I_0\sigma_1}{2\mu_1}(\mu_a Z_0)E_2(\mu_a Z_0)+\kappa_a\frac{I_0\sigma_1}{2\mu_1}(\mu_a Z_0)E_1(\mu_a Z_0)
$$

$$+\frac{I_0}{2}\left(\frac{\sigma_2}{\mu_2}-\frac{\sigma_1}{\mu_1}\right)(\mu_a Z_0+\mu_1 d)E_2(\mu_a Z_0+\mu_1 d)$$
$$+\frac{I_0}{2}\left(\frac{\kappa_2\sigma_2}{\mu_2}-\frac{\kappa_1\sigma_1}{\mu_1}\right)(\mu_a Z_0+\mu_1 d)E_2(\mu_a Z_0+\mu_1 d)$$
$$+\frac{I_0}{2}\left(\frac{\sigma_2}{\mu_2}-\frac{\sigma_1}{\mu_1}\right)(\kappa_a\mu_a Z_0+\kappa_1\mu_1 d)E_1(\mu_a Z_0+\mu_1 d). \qquad (14)$$

Several numerical results of intensity-altitude relationships are shown in Fig. 8, in the case of one surface layer. In the calculations of gamma ray intensity from layered half-space, values of constants for each layer should be given independently. We assume that $\mu_1=\mu_2=0.2\,\mathrm{cm}^{-1}$ and $\kappa_1=\kappa_2=1.0$.* As for the constants for air, we used each of two sets, that is, $\mu_a=3.5\times10^{-5}\,\mathrm{cm}^{-1}$ with $\kappa_a=0$, and $\mu_a=4.5\times10^{-5}\,\mathrm{cm}^{-1}$ with $\kappa_a=0.614$. The present calculations were made for four cases, namely, $\sigma_1=0$, $\sigma_1=\sigma_2/2$, $\sigma_1=2\sigma_2$, and $\sigma_2=0$. Thickness of the surface layer was 1 or 10 cm; i. e., $\mu_1 d=0.2$ or 2.0.

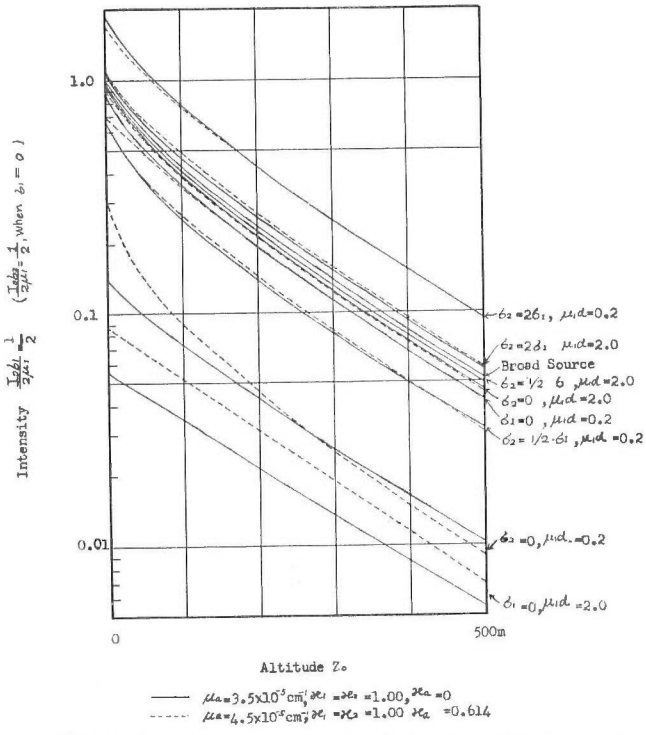


Fig. 8 Effect of surface layers on the intensity-altitude relationship

The intensity-altitude relationships were plotted on a semi-log graph in which abscissa shows altitude and ordinate shows intensity in the log scale. Then, the intensity-altitude curves are approximately represented by straight lines and independent of grade, since the intensities from the extensive sources are nearly proportional to the exponential of altitude. Therefore, the

* These values of constants are derived from the result in Sec. V.3.

gradient of the curve indicates the feature of the intensity-altitude relationship. The gradients of the intensity-altitude curves in Fig. 8 are nearly equal to each other except for those obtained at low altitudes and for two cases of $\mu_1 d=0.2$ with $\sigma_2=0$, and $\mu_1 d=2.0$ with $\sigma_1=0$. In these two extreme cases, the gradient of curves varies with combinations of values of absorption coefficient and scattering constant. A different kind of experiment should be conducted to establish the intensity-altitude relationship, if the thin radioactive layer covering the non-radioactive medium or the thick non-radioactive surface layer is important for practical use. According to the above results, however, a radioactive layer thicker than 10 cm is generally equivalent to a broad source, and therefore, almost all sources are regarded as an infinitely thick source.

### III. 6 Directional Detector

We consider, in this section, the difference in intensity-altitude relationships for a broad source with various directional characters of detector. Here, we consider the cases of two types of directional detector among the four types already referred to in Sec. III. 2.; namely

(1) $I_0$ is replaced by $I_0 \cos\theta$.

(2) $I_0$ is constant for $[0 \leqq \theta \leqq \theta_0, (2\pi-\theta_0) \leqq \theta \leqq 2\pi]$ and zero for $[\theta_0 < \theta < (2\pi-\theta_0)]$,

where $\theta$ is a co-ordinate in the conic co-ordinate system that has an $Z$ axis taken vertical to the broad source. The expressions of gamma ray intensity are given by Eqs. (6) and (9). In the latter case, numerical calculations were performed for $\theta_0=30°$, 45°, and 60°. The results are shown in Fig. 9.

The gradient of the intensity-altitude curve generally decreases with the increase in sensitivity to the vertical component of radiation. The non-direc-

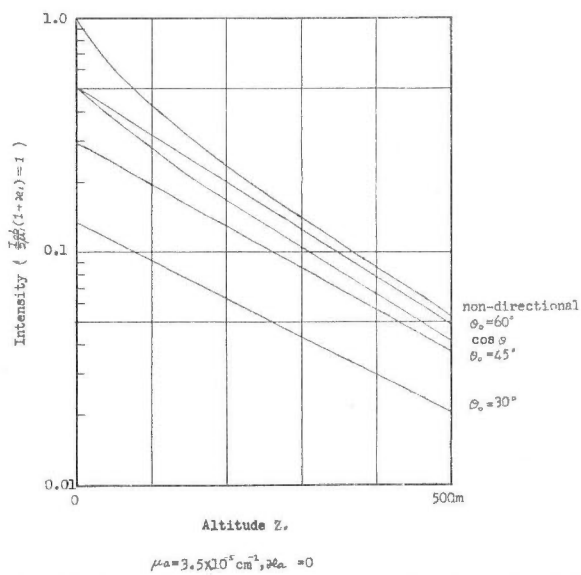


Fig. 9 Effect of directional detectors on the intensity-altitude relationships for the broad source

tional detector will be made less sensitive to altitude changes by shielding the side of the sensitive part, especially at low altitudes.

## IV. Distribution of Gamma Ray Intensity in the Air from Several Sources

### IV. 1 Thick Source

We consider the case of infinitely thick sources with a non-directional detector. A plain polar co-ordinate system $(\rho, \varphi)$ is taken on the surface of the broad source, so that the origin is located at the intersection of a perpendicular through the detector to the surface, as shown in Fig. 10. Length from the detector to any point on the surface is $r_0$.

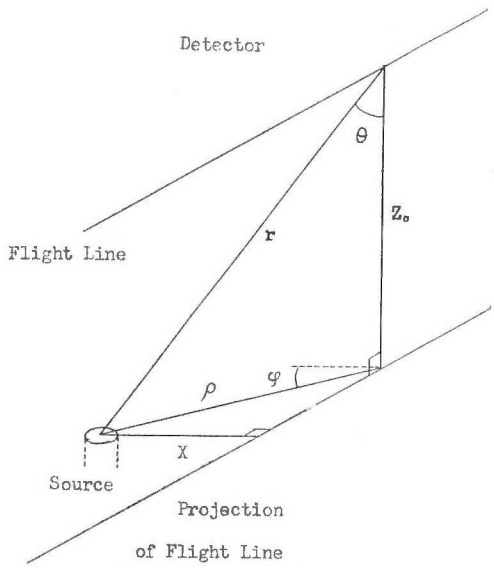


Fig. 10 Small thick source

Then, the expression for the broad source (7) can be rewritten as follows, after integrating with respect to depth in the ground.

$$I^B=\int_0^{\infty}\int_0^{2\pi}\left\{(1+\kappa_1)\frac{I_0\sigma}{\mu_1}\cos\theta\frac{e^{-\mu_a r_0}}{4\pi r_0^2}+\kappa_a\frac{I_0\sigma}{\mu_1}\mu_a r_0\cos\theta\frac{e^{-\mu_a r_0}}{4\pi r_0^2}\right\}\rho d\rho d\varphi,$$

where $\rho d\rho d\varphi$ represents a surface element $dS$. Therefore, we can consider that the radioactive substances in the thick source are condensed to the surface, and the fundamental formula (1) is replaced by

$$I_T=\frac{I_0\sigma}{\mu_1}\left\{(1+\kappa_1)\cos\theta\frac{e^{-\mu_a r_0}}{4\pi r_0^2}+\kappa_a\mu_a r_0\cos\theta\frac{e^{-\mu_a r_0}}{4\pi r_0^2}\right\}dS. \tag{15}$$

This relation is geometrically analogous to the replacement of slab by cone as given in Sec. III.3. As discussed in Sec. III.3 to III.5, Eq. (15) is applicable to many problems concerning airborne surveyings. Gamma ray intensity in air from thick sources can be expressed by integrating Eq. (15), and can

be estimated numerically by using the values of the constant factors, $(1+\kappa_1)I_0\sigma/(2\mu_1)$ and $\kappa_a I_0\sigma/(2\mu_1)$, which are obtained by measurements over a broad source with a certain detector.

Returning the conic co-ordinate $(Z, \theta, \varphi)$, we can reduce Eq. (15) to

$$I_T=\frac{I_0\sigma}{4\pi\mu_1}\left\{(1+\kappa_1)\frac{e^{-\mu_a Z_0\sec\theta}}{\sec^2\theta}+\kappa_a\mu_a Z_0\frac{e^{-\mu_a Z_0\sec\theta}}{\sec\theta}\right\}d(\sec\theta)d\varphi, \tag{16}$$

where $Z_0$ is the height of the detector. Since the thick source can be treated as though it were a radioactive substance condensed to the source surface, it is represented by the areal distribution. If the boundary of the source surface is given by

$$\theta=f(\varphi) \text{ for } [0\leqq\varphi\leqq 2\pi] \text{ or } \theta_1=f_1(\varphi) \text{ and } \theta_2=f_2(\varphi) \text{ for } [\varphi_1\leqq\varphi\leqq\varphi_2],$$

gamma ray intensity $I^T$ from the thick source is written in the following forms.

$$I^T=(1+\kappa_1)\frac{I_0\sigma}{2\mu_1}(\mu_a Z_0)\left\{E_2(\mu_a Z_0)-\frac{2}{\pi}\int_0^{\pi/2}E_2[\mu_a Z_0\sec\{f(\varphi)\}]d\varphi\right\}$$
$$+\kappa_a\frac{I_0\sigma}{2\mu_1}(\mu_a Z_0)\left\{E_1(\mu_a Z_0)-\frac{2}{\pi}\int_0^{\pi/2}E_1[\mu_a Z_0\sec\{f(\varphi)\}]d\varphi\right\},$$

or

$$I^T=(1+\kappa_1)\frac{I_0\sigma}{4\pi\mu_1}(\mu_a Z_0)\int_{\varphi_1}^{\varphi_2}\left\{E_2[\mu_a Z_0\sec\{f_2(\varphi)\}]-E_2[\mu_a Z_0\sec\{f_1(\varphi)\}]\right\}d\varphi$$
$$+\kappa_a\frac{I_0\sigma}{4\pi\mu_1}(\mu_a Z_0)\int_{\varphi_1}^{\varphi_2}\left\{E_1[\mu_a Z_0\sec\{f_2(\varphi)\}]-E_1[\mu_a Z_0\sec\{f_1(\varphi)\}]\right\}d\varphi. \tag{17}$$

These expressions may not be the most convenient for numerical calculation, since, in calculating the difference of $E_n$'s, many decimal figures are necessary. However, they may be useful in out-lining the intensity distribution.

### IV. 2 Source Equivalent to the Broad Source

It may be useful practically to estimate the dimensions of the circular source and the infinite slab source equivalent to the broad source. A circular source is nothing but a cylindrical source embedded in the ground with its

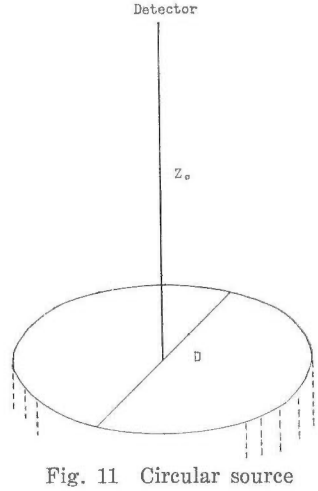


Fig. 11 Circular source

circular end exposed above the ground. If the detector is located on the normal at the center of the circle and the diameter of the circle is $D$, as shown in Fig. 11, gamma ray intensity $I^c$ from the circular source is

$$I^c=(1+\kappa_1)\frac{I_0\sigma}{2\mu_1}(\mu_a Z_0)\{E_2(\mu_a Z_0)-E_2(\mu_a\sqrt{D^2/4+Z_0^2})\}$$
$$+\kappa_a\frac{I_0\sigma}{2\mu_1}(\mu_a Z_0)\{E_1(\mu_a Z_0)-E_1(\mu_a\sqrt{D^2/4+Z_0^2})\}. \quad (18)$$

The results of the estimation for the diameters of circular sources are shown in Fig. 12 as functions of altitude, in which gamma ray intensities amount to 95, 90, and 80%, respectively, of the broad source intensity. Even the diameter of the circular source, from which the intensity is 80% of the broad source intensity, is more than twice as large as the altitude.

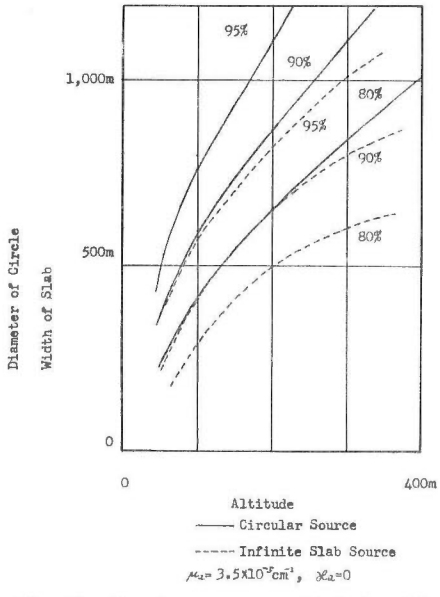


Fig. 12 Circular sources and infinite slab sources equivalent to the broad source

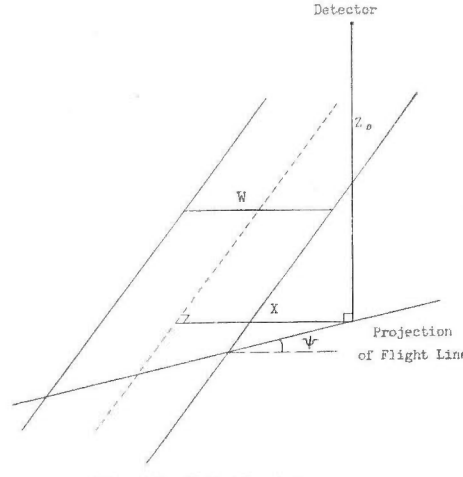


Fig. 13 Infinite slab source

Then, we consider the infinite slab source which extends infinitely in two opposite directions, as shown in Fig. 13. If the detector is located directly over the center line of the source, and the width of the infinite slab is $W$, gamma ray intensity $I^I$ from the source is given by

$$I^I=(1+\kappa_1)\frac{I_0\sigma}{2\mu_1}(\mu_a Z_0)\left[E_2(\mu_a Z_0)-\frac{2}{\pi}\int_0^{\pi/2}E_2\{\mu_a\sqrt{Z_0^2+(W\sec\varphi/2)^2}\}\,d\varphi\right]$$
$$+\kappa_a\frac{I_0\sigma}{2\mu_1}(\mu_a Z_0)\left[E_1(\mu_a Z_0)-\frac{2}{\pi}\int_0^{\pi/2}E_1\{\mu_a\sqrt{Z_0^2+(W\sec\varphi/2)^2}\}\,d\varphi\right]. \quad (19)$$

The widths of the source are estimated for the cases in which gamma ray intensity is 95, 90, and 80%, respectively, of that from the broad source.

The results are shown in Fig. 12 as functions of altitude. The widths thus obtained are comparatively smaller than the diameters of the corresponding circular sources. This may perhaps be due to the fact that the infinite slab source extends infinitely and the areas also are infinite. According to the calculations made by Sakakura[9], the broad source at the altitude of 500 feet, is equivalent to the circular sources that are greater than 1700 feet in diameter and the infinite slab sources which are greater than 1200 feet in width, if these sources, which yield 80% of the broad source intensity, are indistinguishable from the broad source. It is natural that this conclusion nearly coincides with the results shown in Fig. 13, notwithstanding the difference in mathematical expression, since the basic conceptions and fundamental data are analogous.

When a half-space is separated into two parts by a vertical plane boundary, the variation of gamma ray intensity in air across the boundary is easily found. Given the grades in two parts by $\sigma_1$ and $\sigma_2$, absorption coefficients by $\mu_1$ and $\mu_2$, and scattering constants by $\kappa_1$ and $\kappa_2$, respectively, and the ground distance of the detector from the boundary line as $x$, we have

$$
\begin{aligned}
I^{B''}=&\left[\{(1+\kappa_1)\pm(1+\kappa_1)\}\frac{I_0\sigma_1}{4\mu_1}+\{(1+\kappa_2)\mp(1+\kappa_2)\}\frac{I_0\sigma_2}{4\mu_2}\right](\mu_a Z_0)E_2(\mu_a Z_0)\\
&+\left\{\mp(1+\kappa_1)\frac{I_0\sigma_1}{2\pi\mu_1}\pm(1+\kappa_2)\frac{I_0\sigma_2}{2\pi\mu_2}\right\}(\mu_a Z_0)\int_0^{\pi/2}E_2(\mu_a\sqrt{Z_0^2+x^2\sec^2\varphi})d\varphi\\
&+\kappa_a\left[(1\pm1)\frac{I_0\sigma_1}{4\mu_1}+(1\pm1)\frac{I_0\sigma_2}{4\mu_2}\right](\mu_a Z_0)E_1(\mu_a Z_0)\\
&+\left(\mp\frac{I_0\sigma_1}{2\pi\mu_1}\pm\frac{I_0\sigma_2}{2\pi\mu_2}\right)(\mu_a Z_0)\int_0^{\pi/2}E_1(\mu_a\sqrt{Z_0^2+x^2\sec^2\varphi})d\varphi\Bigg].
\end{aligned}
\tag{20}
$$

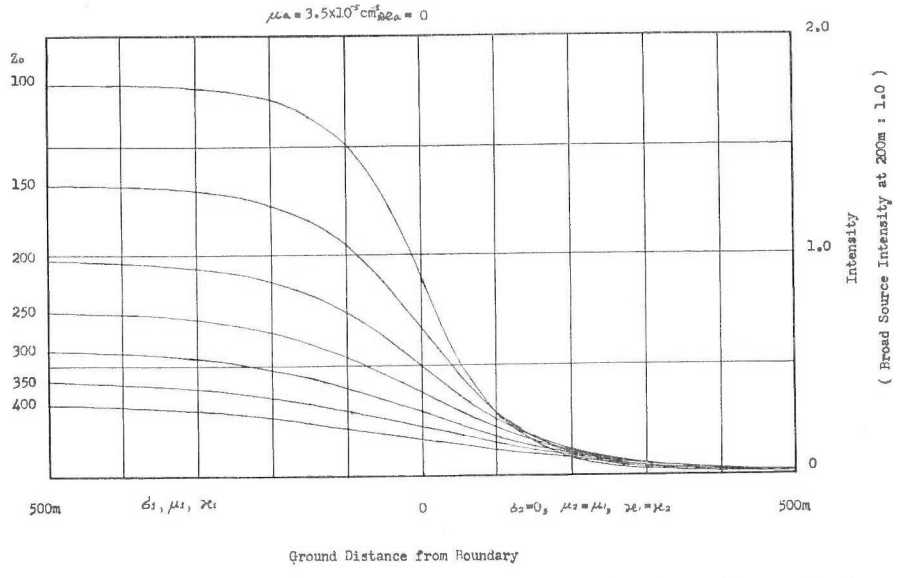


Fig. 14 Variations of gamma ray intensities over the boundary of two effective broad sources

The numerical results are shown in Fig. 14 in the case where $\mu_a=3.5\times10^{-5}\text{cm}^{-1}$, $\kappa_a=0$, and $\sigma_2=0$. The distribution is actually seen when the flight lines cross the coast line perpendicularly of a constant altitude. The intensity-altitude relationship over the vicinity of the boundary is clearly different from that for the broad source.

### IV. 3 Small Thick Source

Gamma ray intensity from a small thick source, that is an infinitely thick source of small surface area can be calculated directly Eq. (15) or (16). The intensity-altitude relationship directly over the elementary slab source is obtained by the integral in Sec. III.3 Eq. (12) is approximately expressed by

$$I^S=\frac{I_0\sigma}{4\pi\mu_1}\left[(1+\kappa_1)\frac{e^{-\mu_a Z_0}}{Z_0^2}+\kappa_a\mu_a Z_0\frac{e^{-\mu_a Z_0}}{Z_0^2}\right]\cdot 4A^2, \tag{21}$$

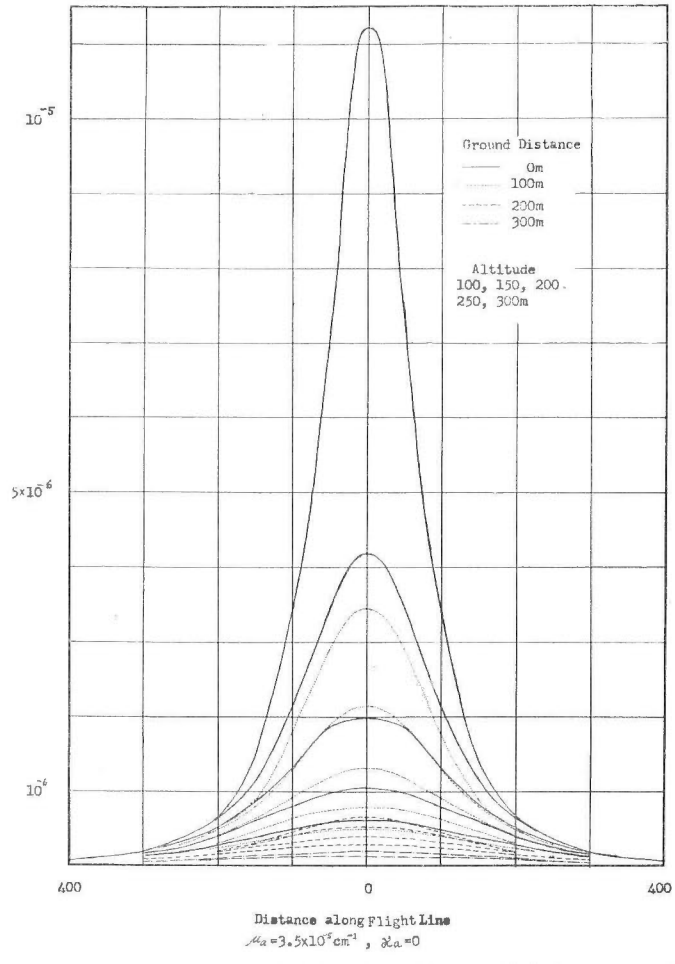


Fig. 15 Intensity distributions from the small thick source of one square meter

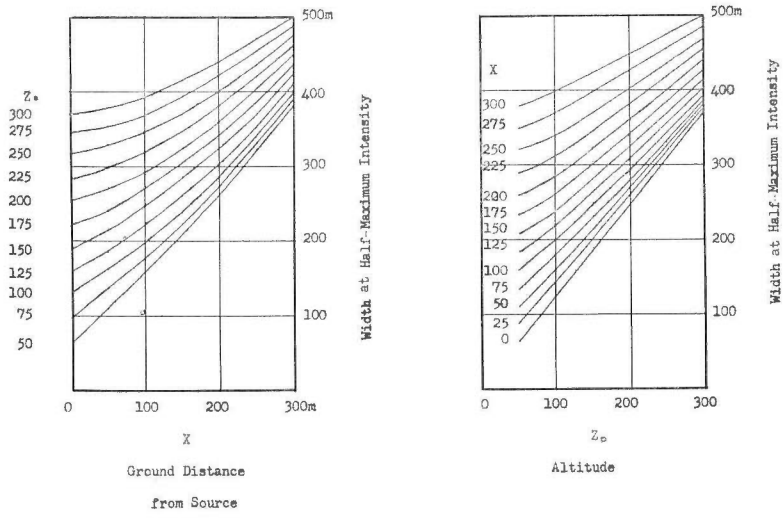


Fig. 16 Width at half-maximum intensity from small thick source

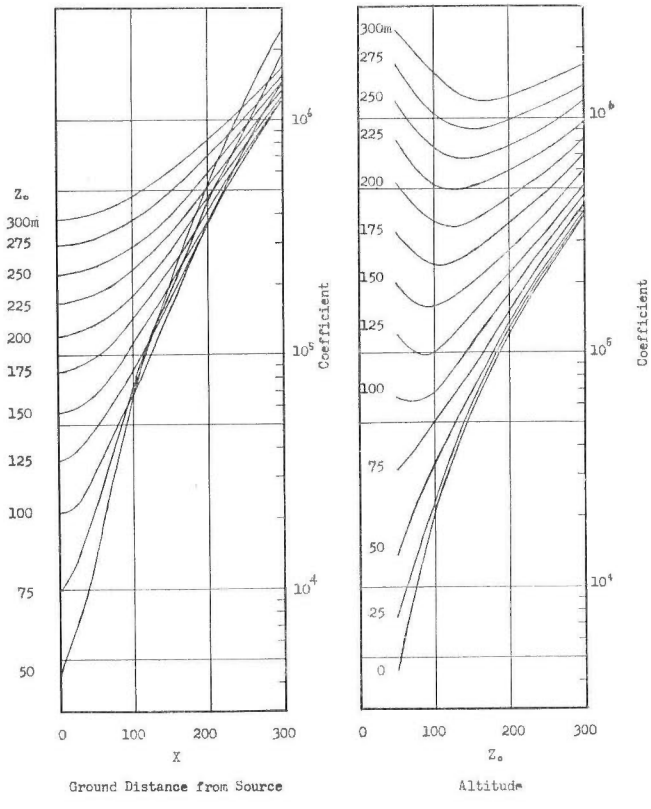


Fig. 17 Coefficient reducing the maximum intensity from the small thick source of one square meter to the broad source intensity at 200m

where $2A$ is the side length of the square surface. It is numerically confirmed that the above formula is a good approximation in the case of the actual elementary slab source, whose area is 145 sq. m the detector being at altitudes higher than 50 m.

The distributions of gamma ray intensity from a thick small source of which the surface area was one square meter are calculated for the case that $\mu_a=3.5\times10^{-5}\,\mathrm{cm}^{-1}$ and $\kappa_a=0$. Examples of the distributions are illustrated in Fig. 15, the detector moving along a straight line at constant altitudes. Minimum ground distance of the detector path, namely, the perpendicular from the center of the source to the projection of the flight line is denoted by $x$, as shown in Fig. 10. Among several characteristics of intensity distribution, the widths at half-maximum intensity and the maximum intensity are easily deduced from the counting rate curve. The widths at half-maximum intensity are shown in Fig. 16 as functions of ground distance or altitude, while the ratios of maximum intensity to the broad source intensity at 200m* from the terrain are shown in Fig. 17 as functions of ground distance or altitude. When the altitude of flight line is constant as known by, for instance, the radio-altimeter record, the ground distance of the flight line from the source is estimated by using Fig. 16. Then the grade of the broad source by using the coefficient estimated from Fig. 17 substitutes for the product of the grade and the surface area of a small thick source. As pointed out,[9] the width at half-maximum intensity may not be suitable for quantitative analysis. However, the charts obtained may be useful for a rough evaluation from the observation along a flight line. In order to estimate the grade and the source area independently, it is necessary to observe anomalous gamma ray intensity from one source in two adjacent flight lines, so as to determine the shape of surface or the source type.

The limits for distinguishable area of effective small thick source are minimum for definite altitudes when the detector is directly over the source. This limit for a circular source is estimated and is expressed roughly by $0.2\ Z_0^2$, that is, $0.5\ Z_0$ in diameter, for the altitude range from 50 to 200m, assuming that the deviation of intensity calculated by (16) from that by Eq. (19), is less than 5 %.

### IV. 4 Infinite Slab Source

The gamma ray intensity $I^I$ from the infinite slab source at ground distance $x$ from the center line of the source, of which the width is $W$, is expressed as

$$I^I=(1+\kappa_1)\ \frac{I_0\sigma}{2\pi\mu_1}(\mu_a Z_0)\int_0^{\pi/2}\Big\{E_2(\mu_a\sqrt{Z_0^2+(2x-W)^2\sec^2\varphi/4}\ )$$
$$-E_2(\mu_a\sqrt{Z_0^2+(2x+W)^2\sec^2\varphi/4})\Big\}d\varphi$$
$$+\kappa_a\frac{I_0\sigma}{2\pi\mu_1}(\mu_a Z_0)\int_0^{\pi/2}\Big\{E_1(\mu_a\sqrt{Z_0^2+(2x-W)^2\sec^2\varphi/4}\ )$$

* Gamma ray intensities in the air are compared with the reducing intensities at the altitude of 200 m in routine work at the Geological Survey of Japan, because of the lack of the experimental data at very low altitudes.

$$-E_1(\mu_a\sqrt{Z_0^2+(2x+W)^2}\sec^2\varphi/4)\Big\}d\varphi, \tag{22}$$

when $2x \geqq W$, and

$$I^I=(1+\kappa_1)\frac{I_0\sigma}{2\mu_1}(\mu_a Z_0)\Big[E_2(\mu_a Z_0)-\frac{1}{\pi}\int_0^{\pi/2}\Big\{E_2(\mu_a\sqrt{Z_0^2+(2x-W)^2}\sec^2\varphi/4)$$
$$+E_2(\mu_a\sqrt{Z_0^2+(2x+W)^2}\sec^2\varphi/4)\Big\}d\varphi\Big]$$
$$+\kappa_a\frac{I_0\sigma}{2\mu_1}(\mu_a Z_0)\Big[E_1(\mu_a Z_0)-\frac{1}{\pi}\int_0^{\pi/2}\Big\{E_1(\mu_a\sqrt{Z_0^2+(2x-W)^2}\sec^2\varphi/4)$$
$$+E_1(\mu_a\sqrt{Z_0^2+(2x+W)^2}\sec^2\varphi/4)\Big\}d\varphi\Big], \tag{23}$$

when $2x < W$.

Numerical calculations were carried out in the case of $\mu_a=3.5\times10^{-5}\,\mathrm{cm}^{-1}$ with $\kappa_a=0$. The examples are illustrated in Fig. 18, the flight line being perpendicular to the source, and the flight level remaining constant. The width at half-maximum intensity and the ratio of maximum intensity to the

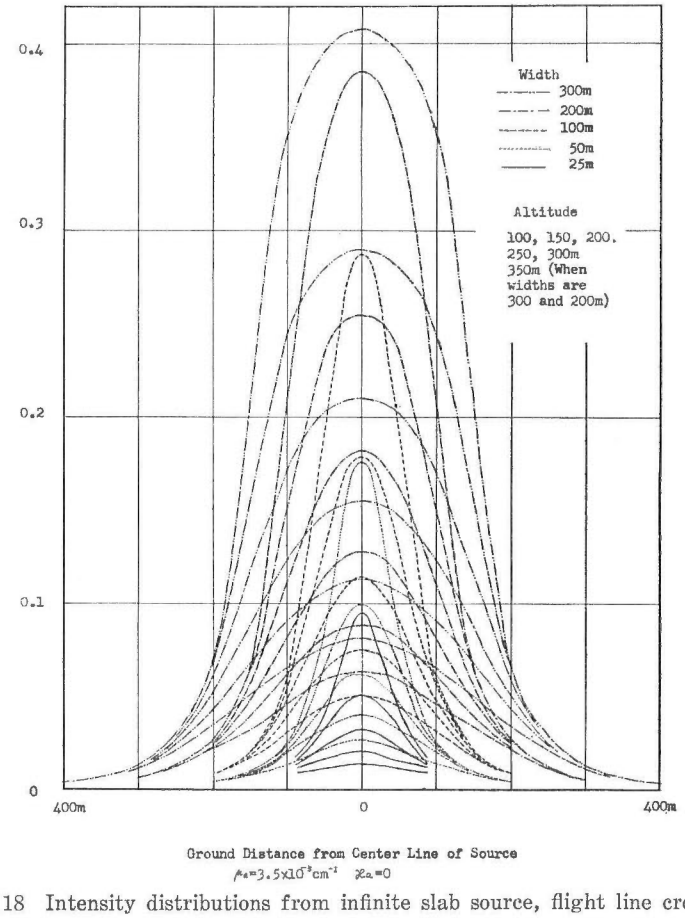


Fig. 18 Intensity distributions from infinite slab source, flight line crossing the source perpendicularly

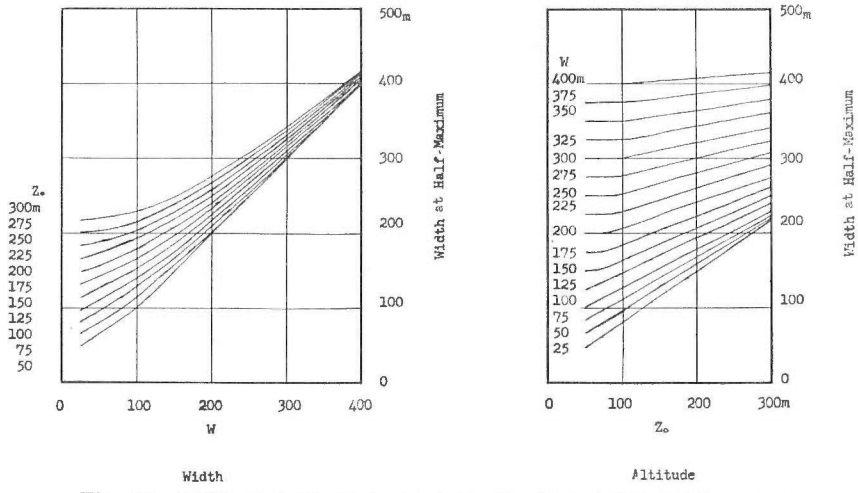


Fig. 19 Width at half-maximum intensity from infinite slab source

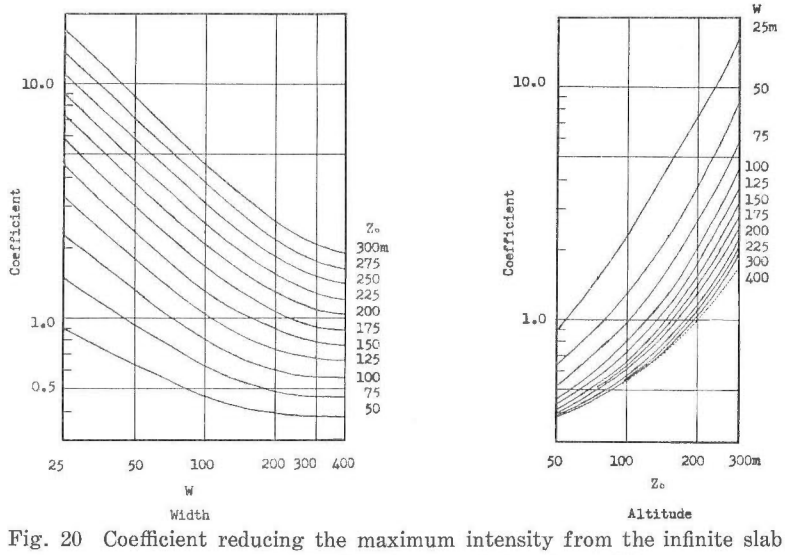


Fig. 20 Coefficient reducing the maximum intensity from the infinite slab source to the broad source intensity at 200 m

broad source intensity at 200 m from the terrain are shown in Figs. 19 and 20, respectively, as functions of the source width and altitude. In the case of oblique cross flight over the slab source, when the angle between the flight line and the center line of source is $\Psi$, as shown in Fig. 13, we have an expression similar with the above formulae in which $x \sec\Psi$ or $W\sec\Psi$ substitutes for $x$ or $W$, respectively, for the intensity distribution along the flight line.

If the angle $\Psi$ from the counting rate curves obtained along the adjacent flight lines is determined, the value of $W \sec\Psi$ is estimated by using the curves in Fig. 19. Then, the grade of the source is deduced from the grade of the broad source. The width at half-maximum intensity represents the

value of $W \sec \Psi$ when the altitude is low compared with $W \sec \Psi$.

### IV. 5 Topographic Effect

In airborne surveyings, flight levels are forced to change over regions of rough topography. The topographic effect hitherto considered is the variation in intensity corresponding to change in altitude. It is, therefore, thought necessary to take into consideration the effect of wavy topography, besides the mere altitude correction, in order to make possible the comparison with the actual grades in rocks distributed in mountainous regions. We shall now estimate the gamma ray intensity measured by non-directional detector over several different topographies uniformly, filled with radioactive substances.

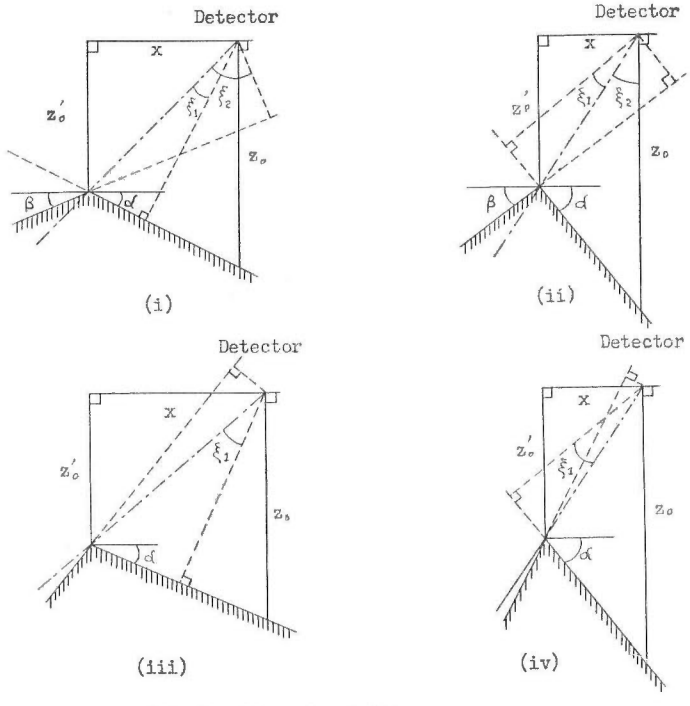


(1) Two Dimensional Ridge

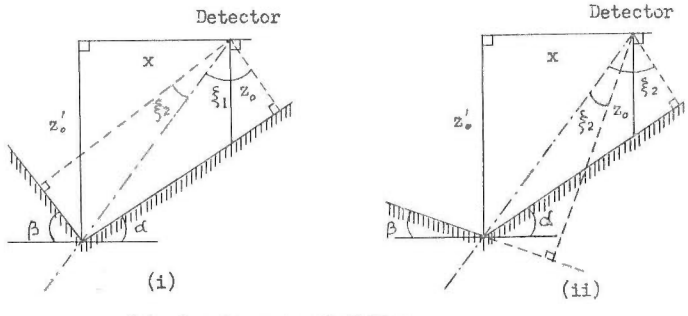


(2) Two Dimensional Valley

Fig. 21 Two dimensional topographies

We now consider the two dimensional ridge or valley formed by simple slopes, as shown in Fig. 21. Gamma ray intensity from these ridges and valleys is obtained by combining the integrals for infinite slab sources which are of infinite width on either side.

Additional symbols used in the calculations are as follows:

$I^R$ or $I^V$: gamma ray intensity from a typical ridge or a typical valley, respectively

$Z_0'$: height of the horizontal plane through the detector from the top of the ridge or the bottom of the valley

$\alpha$ and $\beta$: angles between the horizontal plane and the plane surface forming a ridge or a valley

$\xi_1$ and $\xi_2$: angle that the plane which contains the detector and the intersections of two surfaces makes with the plane which contains the detector and the perpendicular from the detector to the surface

$x$: horizontal distance of the detector to the intersections of the two surfaces

**Two dimensional ridge**

(1) When the extension of the plane, which contains the detector and the top of the ridge passes over the terrain, and when the two perpendiculars from the detector to the surfaces exist on either side of the plane above described, we have

$$\tan\xi_1=\frac{x\cos\alpha-Z_0'\sin\alpha}{x\sin\alpha+Z_0'\cos\alpha},\qquad \tan\xi_2=\frac{x\cos\beta+Z_0'\sin\beta}{Z_0'\cos\beta-x\sin\beta}. \tag{24}$$

Then, we get

$$\begin{aligned}
I^R=&\int_{Z_0\cos\alpha}^{\infty}\int_{-\sqrt{1+\sec^2\varphi\tan^2\xi_1}}^{\infty}\int_0^{\pi} I'dZd(\sec\theta)d\varphi\\
&+\int_{Z_0'\cos\beta-x\sin\beta}^{\infty}\int_{\sqrt{1+\sec^2\varphi\tan^2\xi_2}}^{\infty}\int_0^{\pi} I'dZd(\sec\theta)d\varphi\\
=&(1+\kappa_1)\frac{I_0\sigma}{2\mu_1}\Bigg\{(\mu_aZ_0\cos\alpha)E_2(\mu_aZ_0\cos\alpha)\\
&-\frac{1}{\pi}\int_0^{\pi/2}\{(\mu_aZ_0\cos\alpha)E_2(\mu_aZ_0\cos\alpha\sqrt{1+\sec^2\varphi\tan^2\xi_1})\}d\varphi\\
&+\frac{1}{\pi}\int_0^{\pi/2}[(\mu_a(Z_0'\cos\beta-x\sin\beta)E_2\{\mu_a(Z_0'\cos\beta-x\sin\beta)\sqrt{1+\sec^2\varphi\tan^2\xi_2}\}]d\varphi\Bigg\}\\
&+\kappa_a\frac{I_0\sigma}{2\mu_1}\Bigg\{(\mu_aZ_0\cos\alpha)E_1(\mu_aZ_0\cos\alpha)\\
&-\frac{1}{\pi}\int_0^{\pi/2}\{(\mu_aZ_0\cos\alpha)E_1(\mu_aZ_0\cos\alpha\sqrt{1+\sec^2\varphi\tan^2\xi_1})\}d\varphi\\
&+\frac{1}{\pi}\int_0^{\pi/2}[\mu_a(Z_0'\cos\beta-x\sin\beta)E_1\{\mu_a(Z_0'\cos\beta-x\sin\beta)\sqrt{1+\sec^2\varphi\tan^2\xi_2}\}]d\varphi\Bigg\}.
\end{aligned} \tag{25}$$

(2) When the plane which contains the detector and the top of the ridge passes over the ground, and the two perpendiculars from the detector to the surfaces exist on each side of the plane above described,

$$\tan\xi_1=\frac{Z_0'\sin\alpha-x\cos\alpha}{x\sin\alpha+Z_0'\cos\alpha},\qquad \tan\xi_2=\frac{x\cos\beta+Z_0'\sin\beta}{Z_0'\cos\beta-x\sin\beta}. \tag{26}$$

Then, we have

$$I^R=\int_{Z_0\cos\alpha}^{\infty}\int_{\sqrt{1+\sec^2\varphi\tan^2\xi_1}}^{\infty}\int_0^{\pi} I'dZd(\sec\theta)d\varphi$$
$$+\int_{Z_0'\cos\beta-x\sin\beta}^{\infty}\int_{\sqrt{1+\sec^2\varphi\tan^2\xi_2}}^{\infty}\int_0^{\pi} I'dZd(\sec\theta)d\varphi$$
$$=(1+\kappa_1)\frac{I_0\sigma}{2\pi\mu_1}\int_0^{\pi/2}[(\mu_aZ_0\cos\alpha)E_2(\mu_aZ_0\cos\alpha\sqrt{1+\sec^2\varphi\tan^2\xi_1})$$
$$+\{\mu_a(Z_0'\cos\beta-x\sin\beta)\}E_2\{\mu_a(Z_0'\cos\beta-x\sin\beta)\sqrt{1+\sec^2\varphi\tan^2\xi_2}\}]d\varphi$$
$$+\kappa_a\frac{I_0\sigma}{2\pi\mu_1}\int_0^{\pi/2}[(\mu_aZ_0\cos\alpha)E_1(\mu_aZ_0\cos\alpha\sqrt{1+\sec^2\varphi\tan^2\xi_1})$$
$$+\{\mu_a(Z_0'\cos\beta-x\sin\beta)\}E_1\{\mu_a(Z_0'\cos\beta-x\sin\beta)\sqrt{1+\sec^2\varphi\tan^2\xi_2}\}]d\varphi. \quad (27)$$

(3) When the plane which contains the detector and the top of the ridge does not pass over the terrain and the two perpendiculars from the detector to the surfaces exist on each side of the plane above described, we have

$$\tan\xi_1=\frac{x\cos\alpha-Z_0'\sin\alpha}{x\sin\alpha+Z_0'\cos\alpha}. \quad (28)$$

Then, we get

$$I^R=\int_{Z_0\cos\alpha}^{\infty}\int_{-\sqrt{1+\sec^2\varphi\tan^2\xi_1}}^{\infty}\int_0^{\pi} I'\,dZd(\sec\varphi)d\varphi$$
$$=(1+\kappa_1)\frac{I_0\sigma}{2\mu_1}\left\{(\mu_aZ_0\cos\alpha)E_2(\mu_aZ_0\cos\alpha)\right.$$
$$\left.-\frac{1}{\pi}\int_0^{\pi/2}\{(\mu_aZ_0\cos\alpha)E_2(\mu_aZ_0\cos\alpha\sqrt{1+\sec^2\varphi\tan^2\xi_1})\}d\varphi\right\}$$
$$+\kappa_a\frac{I_0\sigma}{2\mu_1}\left\{(\mu_aZ_0\cos\alpha)E_1(\mu_aZ_0\cos\alpha)\right.$$
$$\left.-\frac{1}{\pi}\int_0^{\pi/2}\{(\mu_aZ_0\cos\alpha)E_1(\mu_aZ_0\cos\alpha\sqrt{1+\sec^2\varphi\tan^2\xi_1})\}\,d\varphi\right\}. \quad (29)$$

Both in the above and in the following cases, we neglect the decrease in gamma ray intensity caused by the space bounded by one surface of the ridge and the plane which contains the detector and the top of the ridge. So far as the ridge is regarded as a thick source, except for the neighbourhood of top, the above approximation may be valid.

(4) When the plane which contains the detector and the top of the ridge does not pass over the terrain, and the two perpendiculars from the detector to the surfaces exist on either side of the plane above described, we have

$$\tan\xi_1=\frac{Z_0'\sin\alpha-x\cos\alpha}{x\sin\alpha+Z_0'\cos\alpha}. \quad (30)$$

Then, we get

$$I^R=\int_{Z_0\cos\alpha}^{\infty}\int_{\sqrt{1+\sec^2\varphi\tan^2\xi_1}}^{\infty}\int_0^{\pi} I'\,dZd(\sec\theta)d\varphi$$
$$=(1+\kappa_1)\frac{I_0\sigma}{2\pi\mu_1}\int_0^{\pi/2}(\mu_aZ_0\cos\alpha)E_2(\mu_aZ_0\cos\alpha\sqrt{1+\sec^2\varphi\tan^2\xi_1})d\varphi$$
$$+\kappa_a\frac{I_0\sigma}{2\pi\mu_1}\int_0^{\pi/2}(\mu_aZ_0\cos\alpha)E_1(\mu_aZ_0\cos\alpha\sqrt{1+\sin^2\varphi\tan^2\xi_1})d\varphi. \quad (31)$$

**Two dimensional valley**

(1) When the two perpendiculars from the detector to the surfaces exist on each side of the plane, which contains the detector and bottom of the valley, we have

$$\tan\xi_1=\frac{x\cos\alpha+Z_0'\sin\alpha}{Z_0'\cos\alpha-x\sin\alpha},\qquad \tan\xi_2=\frac{Z_0'\sin\beta-x\cos\beta}{x\sin\beta+Z_0'\cos\beta}. \tag{32}$$

Then, we get

$$\begin{aligned}
I^V=&\int_{Z_0\cos\alpha}^{\infty}\int_{-\sqrt{1+\sec^2\varphi\tan^2\xi_1}}^{\infty}\int_0^{\pi} I'dZd(\sec\theta)d\varphi\\
&+\int_{Z_0'\cos\beta+x\sin\beta}^{\infty}\int_{-\sqrt{1+\sec^2\varphi\tan^2\xi_2}}^{\infty}\int_0^{\pi} I'dZd(\sec\theta)d\varphi\\
=&(1+\kappa_1)\frac{I_0\sigma}{2\mu_1}\Big\{(\mu_aZ_0\cos\alpha)E_2(\mu_aZ_0\cos\alpha)\\
&-\frac{1}{\pi}\int_0^{\pi/2}\{(\mu_aZ_0\cos\alpha)E_2(\mu_aZ_0\cos\alpha\sqrt{1+\sec^2\varphi\tan^2\xi_1})\}d\varphi\\
&+\mu_a(Z_0'\cos\beta+x\sin\beta)E_2\{\mu_a(Z_0'\cos\beta+x\sin\beta)\}\\
&-\frac{1}{\pi}\int_0^{\pi/2}[\mu_a(Z_0'\cos\beta+x\sin\beta)E_2\{\mu_a(Z_0'\cos\beta+x\sin\beta)\sqrt{1+\sec^2\varphi\tan^2\xi_2}\}]\,d\varphi\Big\}\\
&+\kappa_a\frac{I_0\sigma}{2\mu_1}\Big\{(\mu_aZ_0\cos\alpha)E_1(\mu_aZ_0\cos\alpha)\\
&-\frac{1}{\pi}\int_0^{\pi/2}\{(\mu_aZ_0\cos\alpha)E_1(\mu_aZ_0\cos\alpha\sqrt{1+\sec^2\varphi\tan^2\xi_1})\}d\varphi\\
&+\mu_a(Z_0'\cos\beta+x\sin\beta)E_1\{\mu_a(Z_0'\cos\beta+x\sin\beta)\}\\
&-\frac{1}{\pi}\int_0^{\pi/2}[\mu_a(Z_0'\cos\beta+x\sin\beta)E_1\{\mu_a(Z_0'\cos\beta+x\sin\beta)\sqrt{1+\sec^2\varphi\tan^2\xi_2}\}]d\varphi\Big\}.
\end{aligned} \tag{33}$$

(2) When the two perpendiculars from the detector to the surfaces exist on either side of the plane, which contains the detector and the bottom of the valley, we have

$$\tan\xi_1=\frac{x\cos\alpha+Z_0'\sin\alpha}{Z_0'\cos\alpha-x\sin\alpha},\qquad \tan\xi_2=\frac{x\cos\beta-Z_0'\sin\beta}{x\sin\beta+Z_0'\cos\beta}. \tag{34}$$

Then, we get

$$\begin{aligned}
I^V=&\int_{Z_0\cos\alpha}^{\infty}\int_{-\sqrt{1+\sec^2\varphi\tan^2\xi_1}}^{\infty}\int_0^{\pi} I'dZd(\sec\theta)d\varphi\\
&+\int_{Z_0'\cos\beta+x\sin\beta}^{\infty}\int_{\sqrt{1+\sec^2\varphi\tan^2\xi_2}}^{\infty}\int_0^{\pi} I'dZd(\sec\theta)d\varphi\\
=&(1+\kappa_1)\frac{I_0\sigma}{2\mu_1}\Big\{(\mu_aZ_0\cos\alpha)E_2(\mu_aZ_0\cos\alpha)\\
&-\frac{1}{\pi}\int_0^{\pi/2}(\mu_aZ_0\cos\alpha)E_2(\mu_aZ_0\cos\alpha\sqrt{1+\sec^2\varphi\tan^2\xi_1})d\varphi\\
&+\frac{1}{\pi}\int_0^{\pi/2}\mu_a(Z_0'\cos\beta+x\sin\beta)E_2\{\mu_a(Z_0'\cos\beta+x\sin\beta)\sqrt{1+\sec^2\varphi\tan^2\xi_2}\}\,d\varphi\Big\}\\
&+\kappa_a\frac{I_0\sigma}{2\mu_1}\Big\{(\mu_aZ_0\cos\alpha)E_1(\mu_aZ_0\cos\alpha)
\end{aligned}$$

$$-\frac{1}{\pi}\int_0^{\pi/2}(\mu_a Z_0\cos\alpha)\,E_1(\mu_a Z_0\cos\alpha\sqrt{1+\sec^2\varphi\tan^2\xi_1})d\varphi$$
$$+\frac{1}{\pi}\int_0^{\pi/2}\mu_a(Z_0'\cos\beta+x\sin\beta)E_1\{\mu_a(Z_0'\cos\beta+x\sin\beta)\sqrt{1+\sec^2\varphi\tan^2\xi_2}\}d\varphi\Big\}. \tag{35}$$

When the detector is located directly over the top of the ridge or the bottom of the valley, the topographic effect is clearly observable. Therefore, numerical calculations were carried out for the cases above mentioned for the combination of constants that $\mu_a=3.5\times10^{-5}\,\mathrm{cm}^{-1}$ and $\kappa_a=0$ assuming

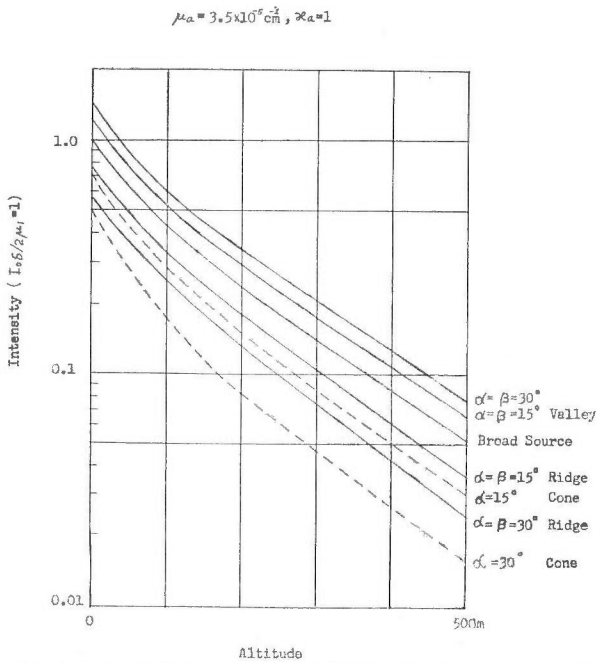


Fig. 22 Intensity-altitude relationships for several topographies

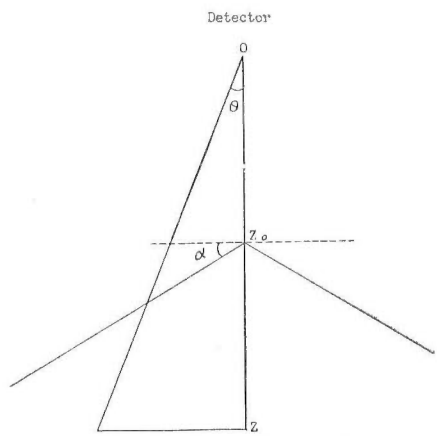


Fig. 23 Cone (Mountain)

$\alpha=\beta$. The results are shown in Fig. 22 in the form of intensity-altitude relationships for several definite values of $\alpha$. It is notable that these intensity-altitude curves are nearly parallel to each other and to the broad source curve, too.

In the next place, the effect of conical topography for an isolated mountain is studied. The detector is located over the top of the mountain and the height of the detector from the top is $Z_0$, as shown in Fig. 23, the gamma ray intensity $I^M$ from the mountain is given by the following formula, the angle between the horizontal plane and the surface of the cone being $\alpha$.

$$I^M=\int_{Z_0\cot\alpha/(\cot\alpha-\tan\theta)}^{\infty}\int_1^{\operatorname{cosec}\alpha}\int_0^{2\pi} I'dZd(\sec\theta)d\varphi$$
$$=(1+\kappa_1)\frac{I_0\sigma}{2\mu_1}\int_0^{\pi/2-\alpha}\exp\left(-\frac{\mu_a Z_0}{\cos\theta-\sin\theta\tan\alpha}\right)\sin\theta\,d\theta$$
$$+\kappa_a\frac{I_0\sigma}{2\mu_1}\int_0^{\pi/2-\alpha}(\mu_a Z_0)\exp\left(-\frac{\mu_a Z_0}{\cos\theta-\sin\theta\tan\alpha}\right)\frac{\sin\theta}{(\cos\theta-\sin\theta\tan\alpha)}d\theta\,. \quad (36)$$

Numerical results are shown in Fig. 22 in which the values of constant employed are $\mu_a=3.5\times10^{-5}\,\mathrm{cm}^{-1}$ with $\kappa_a=0$. The intensity-altitude curves are nearly parallel to the broad source curve, except for those at low altitudes.

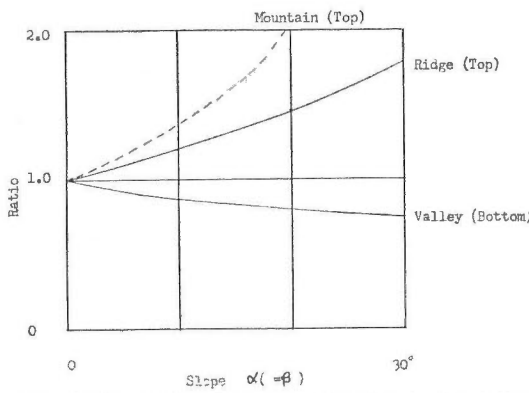


Fig. 24 Ratios of broad source intensity to the intensity from several typical topographies

Therefore, the ratios of the gamma ray intensity affected by typical topographies to the broad source intensity are nearly independent of altitude, although the ratios depend upon the type of topography and the angle of slope. The ratios are shown in Fig. 24 and are regarded as topographic correction factors at the top of the ridge or mountain and at the bottom of the valley.

### IV. 6 Discussions on the Intensity-Altitude Relationship

The apparent variations in gradient of the intensity-altitude curve are derived from the results of the preceding section. When the aircraft flies horizontally across the mountain range perpendicular to the ridge, the intensity-altitude curve, drawn by observed data along the flight line, would be more

or less oblique compared with the broad source curve. This is due to the fact that the altitude above the valley is higher than that above the ridge and that the intensity above the valley is higher than the broad source intensity at the same altitude, while the intensity above the ridge is lower. On the contrary, the curve drawn by the observed data would have the same gradient as the broad source curve, when the flight line is parallel to the direction of the ridge or the valley. Therefore, various gradients in the intensity-altitude curves are obtained from the observed data in mountainous regions.

The apparent variations in gradient are recognized in actual survey data by comparing the intensity variation with the topography along the flight line. The usual altitude correction, which is followed by the broad source curve, may be permissible, since the results of the preceding section indicate that the topographic correction can be approximately made independent of the altitude correction.

Another explanation may be possible for the variations in gradient, besides topographic effects. The radioactivity of granitic rocks usually decreases with the progress of weathering, and therefore, the terrestrial radioactivity increases sometimes as depth below the ground surface increases. On the contrary, the research group on background radiation[4] found that the accumulation of artificial radioactive substances was located in a thin layer of the ground surface. If one remembers the calculations on the effect of surface layer in Sec. III.5, the deviations in gradient from the broad source curve can not be denied.

The variations in gradient might be derived from the time and spatial change in the zero background, in which the change probably was caused by such airborne radioactive substances as radon. The gradient of curves plotted on semi-log graphs depend seriously upon the estimation of the zero background, since the intensity from the terrestrial radioactivity is obtained as the difference between the gross counting rate and the zero background.

When radioactive substances are distributed in air with a homogenous content of $\sigma_a$, gamma ray intensity $I^A$ at the altitude of $Z_0$ is deduced from Eqs. (7) and (13). Then, we have

$$I^A=(1+\kappa_a)\frac{I_0\sigma_a}{2\mu_a}\{2-(\mu_a Z_0)E_2(\mu_a Z_0)\}-\kappa_a\frac{I_0\sigma_a}{2\mu_a}(\mu_a Z_0)E_1(\mu_a Z_0).$$

If the value of $(1+\kappa_1)I_0/(2\mu_1)$ obtained in Sec. III.4 for the detector currently used is applicable to the present case and $\kappa_1$ and $\mu_1$ are 1.0 and 0.2 $cm^{-1}$, respectively, $I_0$ is converted to $6\times10^6$ cps$\cdot$cm$^{-1}\cdot(\mu c/g)^{-1}$, since one percent of the uranium series in equilibrium correspond to $3\times10^{-8}$ $\mu c/g$. As nearly all gamma rays from the uranium series are emitted from the daughters of $^{222}R_n$, the above value is held in the case that the parents of radon are missing. M. Kawano[7] determined the atmospheric radon content at a locality in the Tokyo area to be about $2.4\times10^{-13}$ $\mu c/g$ by careful measurement. Then, the intensity $I^A$ at the altitudes of 0, 200 m and infinity is estimated to be $1.7\times10^2$, $3.0\times10^2$, and $3.4\times10^2$ cps, respectively. The zero background has been determined by the measurement of the counting rate on the sea adjacent survey area, and has never changed throughout the survey flights which have

been carried out for three years. The value is about $2\times10^2$ cps and may be due to the contribution from radon and its daughters. The difference between the estimated and the observed values can be neglected owing to the somewhat bold assumptions. For instance, the formula for $I^A$ varies with the altitude, while the observed zero background is independent of altitude.

It is well known that the range of atmospheric radon content is considerably wide. Therefore, the indirect effect of the zero background on the gradient of the intensity-altitude curve should be remembered. However, knowledge, which can be directly compared with the airborne survey data, concerning such surface layers and radioactivity in the air are so scarce at present that investigation on these two effects has never been sufficiently carried out. E. A. Godby et al[6]. also observed various intensity-altitude relationships and concluded that the various relationships may be attributed to various rock types. We think, however, it may be attributed primarily to the topographic effects, and secondarily to the other two effects above discussed.

## V. Distribution of Gamma Ray Intensity in the Drill Hole from a Horizontal Radioactive Layer

### V. 1 Directional Character of Line Detector

Now we are in a position to discuss the distributions of gamma ray intensity in the drill hole as an application of the fundamental formula (1) to problems concerning the gamma ray attenuation through media of the terrain. Let us take the case of the horizontal layer homogeneously filled with radioactive substances. The theoretical consideration is applicable to radioactivity well logging. Objections may perhaps arise that theoretical consideration is unnecessary in well logging, since the analysis of the radioactivity log is usually, and easily made by comparing the results of experiments in artificial model holes. However, we shall discuss variation in the intensity distributions with detector length and thickness of layer by a simple theoretical treatment and then shall determine the constants in the fundamental formula (1) by utilizing experimental data of an artificial model hole.

In the measurement of gamma ray intensity in the drill holes, the size

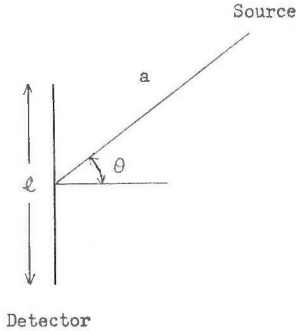


Fig. 25 Line detector

and shape of the detector should be well studied because the detector will pass close to the sources. We considered a line detector whose sensitive part is a line. The length of the detector is $l$ and the sensitivity along the line is uniform. Suppose a point source placed at the distance $a$ from the center of the detector. The line connecting the detector with the source makes an angle $\theta$ with the perpendicular to the detector in the plane, which contains the detector and the source, as shown in Fig. 25. Directional character of the detector is expressed by angular response $I(\theta)$ for the point source, i. e.

$$\theta)=\int_{-l/2}^{l/2}\frac{I_0'd\xi}{(a\tan\theta+\xi)^2}=I_0'\frac{\sec\theta}{4\pi a}\tan^{-1}\left(\frac{ad\cos\theta}{a^2-l^2/4}\right), \tag{37}$$

where $I_0'$ is a constant concerning sensitivity of the detector and the property of the source, and $\xi$ is a co-ordinate along the line detector. The numerical result is shown in Fig. 26, when $l=5$ cm and $a=l$, $2l$ and $3l$. The detector is nearly non-directional at distances of more than three times its length.

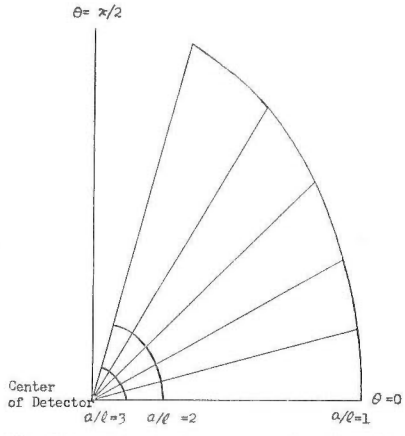


Fig. 26 Directional character of a line detector

Actual detectors used in logging have another kind of directional character which depends upon the absorption by the container of the detector probe, as well as the finiteness of the diameter. The character calculated from the above formula agrees qualitatively with the measurements, at least when the absorption by the container is not remarkable. The substitution of the line detector from the logging detector may be reasonable for the purpose of studying the effects of the detector length.

### V. 2 Horizontal Radioactive Layer

Let us consider the horizontal layer homogeneously filled with radioactive ore. The drill hole discussed in this chapter is dug vertically, and does not contain mud water and casing pipe. We assume that the absorption coefficient and the scattering constant are common to the radioactive layer and the surrounding non-radioactive layers, and that the detector passes through the center of the hole, as shown in Fig. 27. The explanation of symbols is as follows :

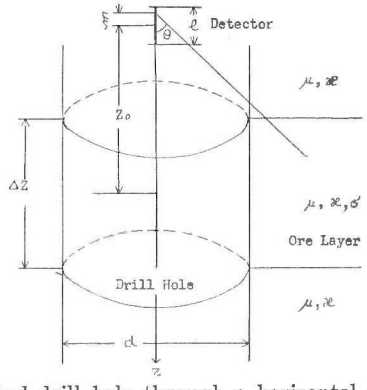


Fig. 27 Vertical drill hole through a horizontal radioactive layer

$I^L$: gamma ray intensity from horizontal ore layer
$I_0$: constant, depending upon the property of source substances and the sensitivity of the detector
$\sigma$: grade of ore
$\mu$: linear absorption coefficient of layers
$\kappa$: scattering constant of layers
$l$: length of the detector
$\xi$: distance along the detector from its center
$d$: diameter of drill hole
$\Delta Z$: thickness of the radioactive layer
$Z_0$: vertical distance between centers of the detector and the radioactive layer
$\theta$: angle which the line connecting the detector to the source makes with the perpendicular to the detector in the plane, which contains the detector and the source

Then, gamma ray intensity from the radioactive layer is expressed by the following integrals.

(1) $Z_0+\xi > \Delta Z/2$

$$I^L=(1+\kappa)\frac{I_0\sigma}{2\mu}\left\{\int_{\tan^{-1}\{d/(2Z_0+2\xi-\Delta Z)\}}^{\pi/2}\int_{-l/2}^{l/2}[\exp\{-\mu(Z_0+\xi-\Delta Z/2-d\cot\theta/2)\sec\theta\}-\exp\{-\mu(Z_0+\xi+\Delta Z/2-d\cot\theta/2)\sec\theta\}]\sin\theta d\theta d\xi+\int_{\tan^{-1}\{d/(2Z_0+2\xi-\Delta Z)\}}^{\tan^{-1}\{d/(2Z_0+2\xi+\Delta Z)\}}\int_{-l/2}^{l/2}[1-\exp\{-\mu(Z_0+\xi+\Delta Z/2-d\cot\theta/2)\sec\theta\}]\sin\theta d\theta d\xi\right\}+\kappa\frac{I_0\sigma}{2\mu}\left\{\int_{\tan^{-1}\{d/(2Z_0+2\xi-\Delta Z)\}}^{\pi/2}\int_{-l/2}^{l/2}[\mu(Z_0+\xi-\Delta Z/2-d\cot\theta/2)\times\exp\{-\mu(Z_0+\xi-\Delta Z/2-d\cot\theta/2)\sec\theta\}-\mu(Z_0+\xi+\Delta Z/2-d\cot\theta/2)\times\exp\{-\mu(Z_0+\xi+\Delta Z/2-d\cot\theta/2)\sec\theta\}]\tan\theta d\theta d\xi-\int_{\tan^{-1}\{d/(2Z_0+2\xi-\Delta Z)\}}^{\tan^{-1}\{d/(2Z_0+2\xi+\Delta Z)\}}\int_{-l/2}^{l/2}\mu(Z_0+\xi+\Delta Z/2-d\cot\theta/2)\times\exp\{-\mu(Z_0+\xi+\Delta Z/2-d\cot\theta/2)\sec\theta\}\tan\theta d\theta d\xi\right\}, \tag{38}$$

(2) $Z_0+\xi \leqq \Delta Z/2$

$$I^L=(1+\kappa)\frac{I_0\sigma}{2\mu}\left\{\int_{\tan^{-1}\{d/(2Z_0+2\xi+\Delta Z)\}}^{\pi/2}\int_{-l/2}^{l/2}[1\right.$$

$$-\exp\{-\mu(Z_0+\xi+\Delta Z/2-d\cot\theta/2)\sec\theta\}]\sin\theta d\theta d\xi+\int_{\tan^{-1}\{d/(2Z_0+2\xi-\Delta Z)\}}^{\pi/2}\int_{-l/2}^{l/2}[1$$

$$-\exp\{-\mu(Z_0+\xi-\Delta Z/2-d\cot\theta/2)\sec\theta\}]\sin\theta\, d\theta\, d\xi\Big\}$$

$$-\kappa\frac{I_0\sigma}{2\mu}\Big\{\int_{\tan^{-1}\{d/(2Z_0+2\xi+\Delta Z)\}}^{\pi/2}\int_{-l/2}^{l/2}[\mu(Z_0+\xi+\Delta Z/2-d\cot\theta/2)$$

$$\times\exp\{-\mu(Z_0+\xi+\Delta Z/2-d\cot\theta/2)\sec\theta\}]\tan\theta\, d\theta\, d\xi$$

$$+\int_{\tan^{-1}\{d/(2Z_0+2\xi-\Delta Z)\}}^{\pi/2}\int_{-l/2}^{l/2}[\mu(Z_0+\xi-\Delta Z/2-d\cot\theta/2)$$

$$\times\exp\{-\mu(Z_0+\xi-\Delta Z/2-d\cot\theta/2)\sec\theta\}]\tan\theta d\theta d\xi\Big\}. \tag{39}$$

When the horizontal radioactive layer is infinitely thick, the integrals are simplified to

$$I^L=(1+\kappa)lI_0\sigma/\mu. \tag{40}$$

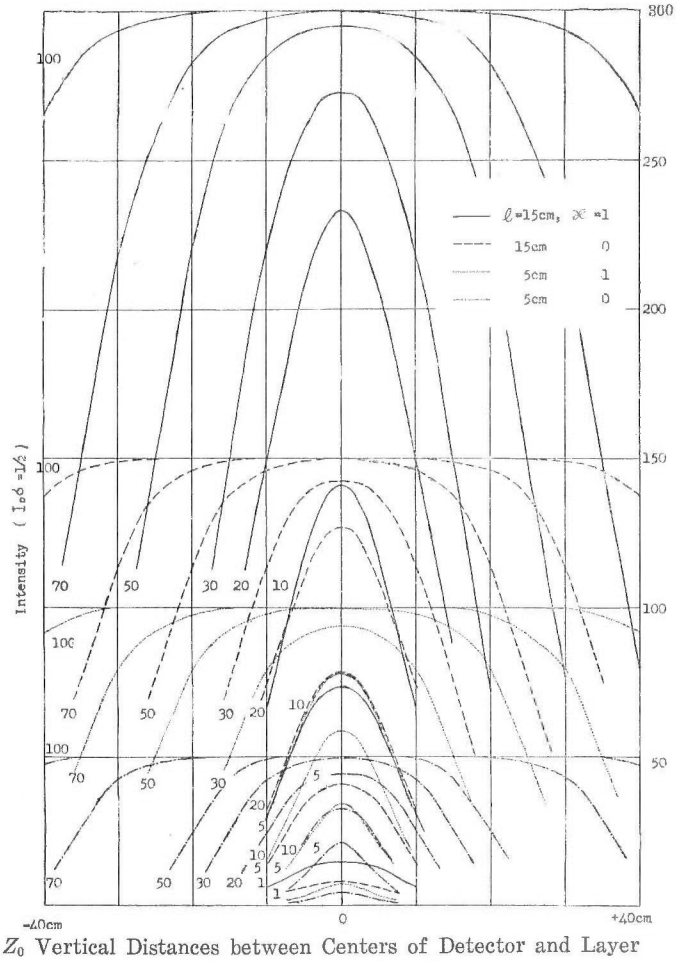


$Z_0$ Vertical Distances between Centers of Detector and Layer
$d=4$ cm $\mu=0.2\,\mathrm{cm}^{-1}$
Figures beside Curve mean Thickness in cm.

Fig. 28
Intensity distributions from horizontal radioactive layers of various thicknesses (I)

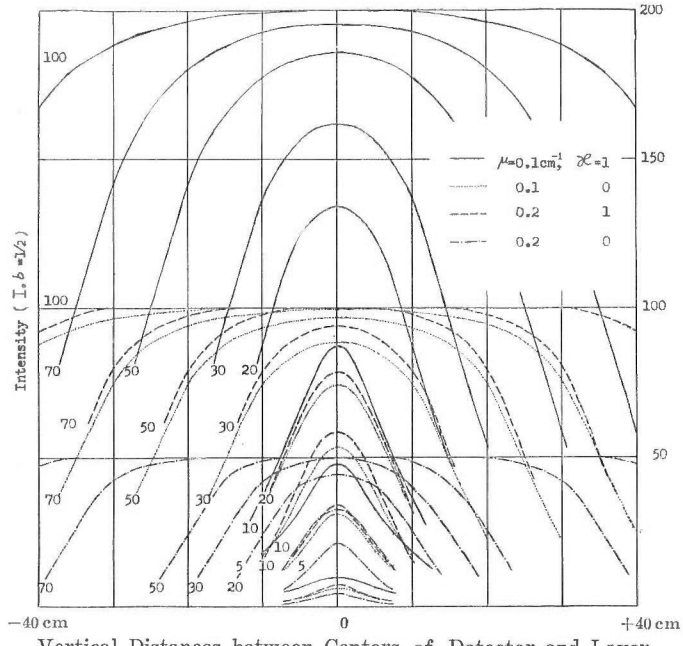


Vertical Distances between Centers of Detector and Layer
$d=4$ cm $l=5$ cm
Figures beside Curve mean Thickness in cm.

Fig. 29

Intensity distributions from horizontal radioactive layers of various thicknesses (II)

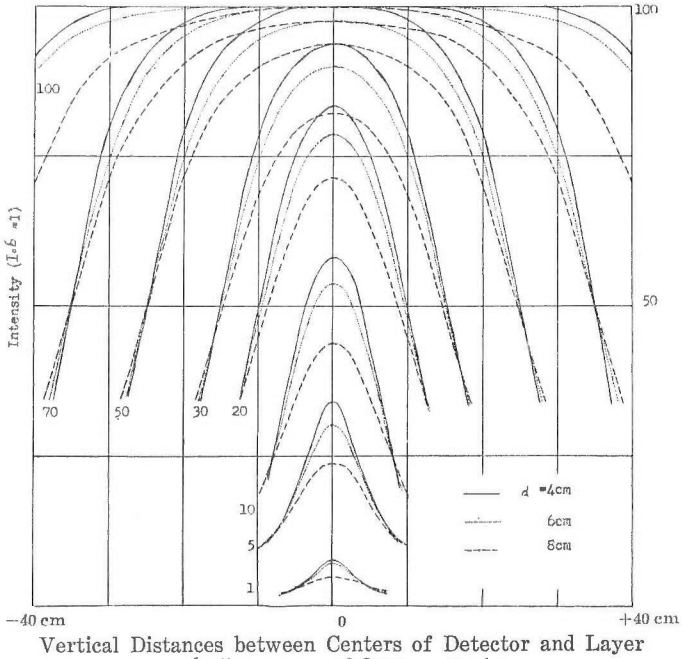


Vertical Distances between Centers of Detector and Layer
$l=5$ cm $\mu=0.2$ cm $\kappa=1$
Figures beside Curve mean Thickness in cm.

Fig. 30

Intensity distributions from horizontal radioactive layers of various thicknesses (III)

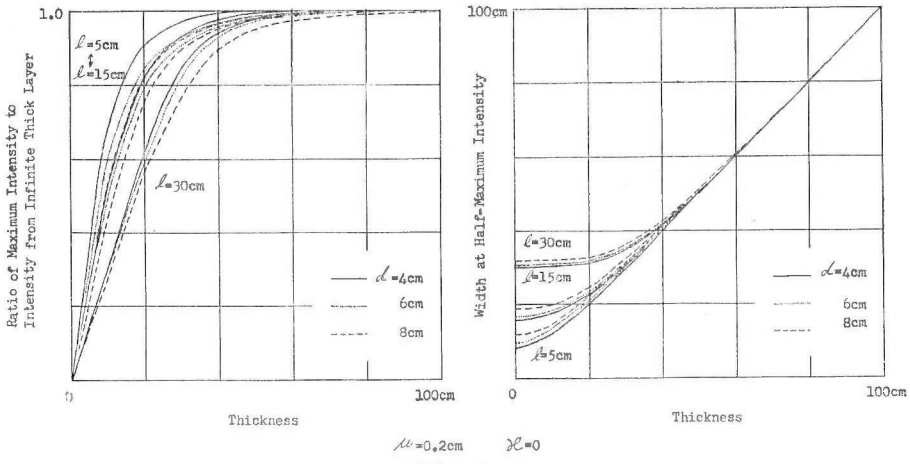


Fig. 31

Characteristics of intensity distributions from horizontal radioactive layers (I)

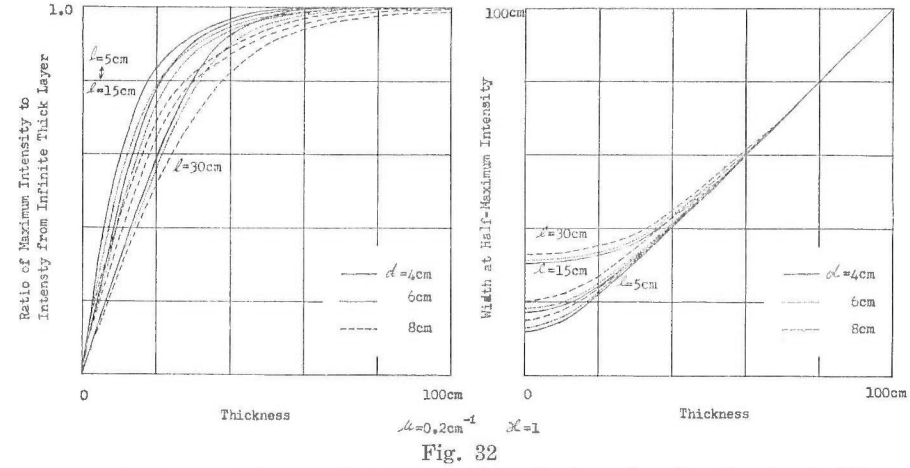


Fig. 32

Characteristics of intensity distributions from horizontal radioactive layers (II)

Numerical evaluations of the above formula were performed in the cases of $l=5$, 15, and 30 cm, and $d=4$, 6, and 8 cm, assuming that $\mu=0.1$ and $0.2\,\mathrm{cm}^{-1}$. Examples of intensity distributions are illustrated in Figs. 28, 29 and 30, when $\kappa=0$ and 1. These figures show the differences in the intensity distributions with the detector length, the absorption coefficient and the diameter of the drill hole, respectively.

Two characteristics of intensity distribution are selected. One is the width at half-maximum intensity and the other is the ratio of maximum intensity to that of the infinitely thick layer. The relationships between the characteristics and the thickness of the layer are shown in Figs. 31, 32, 33 and 34. When the ore bearing layer is sufficiently thick in comparison with the detector length, the width at half-maximum intensity is equal to the thickness, while the ratio approaches unity. On the contrary, the width at

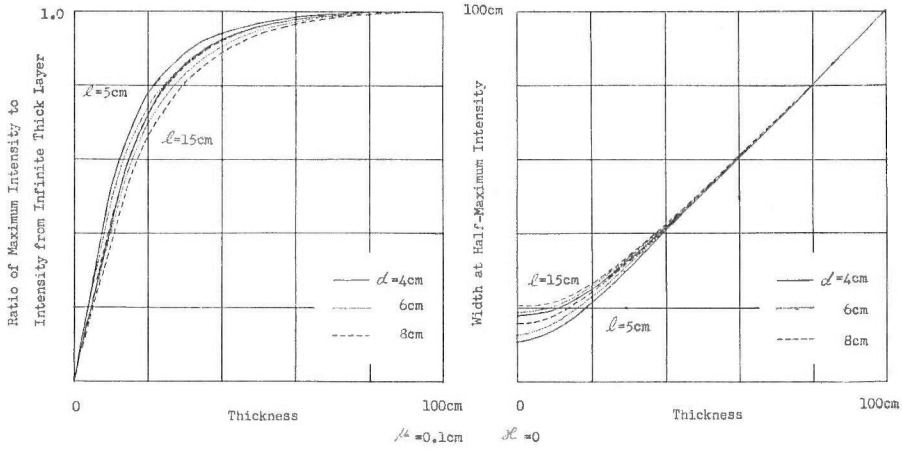


Fig. 33
Characteristics of intensity distributions from horizontal radioactive layers (III)

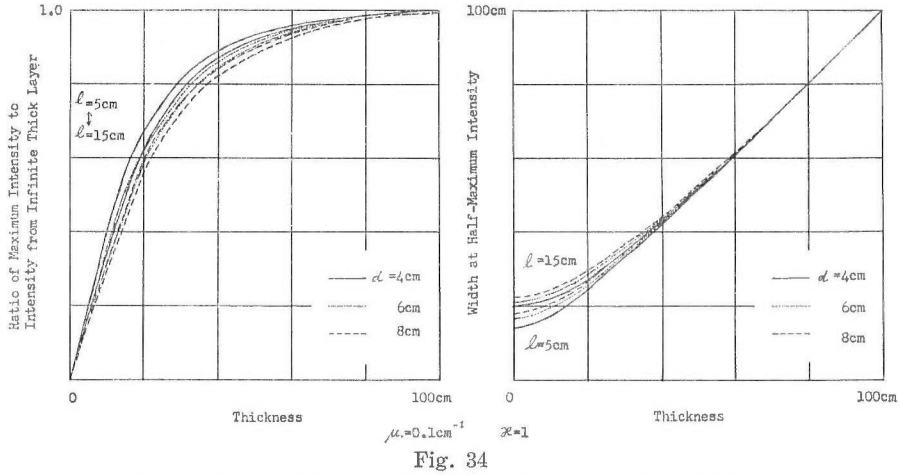


Fig. 34
Characteristics of intensity distributions from horizontal radioactive layers (IV)

half-maximum intensity decreases to minimum and the ratio falls to zero as the thickness of the layer decreases. The minimum of the width at half-maximum intensity depends upon both the detector length and the diameter of the drill hole. In order to find the intensity distribution which clearly indicates the presence of a thin radioactive layer, a small size detector should be used ; but a detector with its length shorter than the diameter of the drill hole may be useless. Consequently, the effects of the detector length expected is drived theoretically.

### V. 3 Determination of Constants

The constant factors in the expressions determining the gamma ray intensity from the horizontal radioactive layer are $I_0\sigma/(2\mu)$ and $\kappa I_0\sigma/(2\mu)$. These values are obtained from the measurement of the gamma ray intensity

in the drill hole from the horizontal ore bearing layer of known thickness, if the proper value of $\mu$ is given. Then, we have the value of $\kappa$.

Some experiments on the measurement of the intensity distributions were made with an artificial model hole which contains two radioactive layers made of ore from the Ningyo Pass Mine. The thicknesses of the ore layers are 5 cm and 43 cm, and the grades are 0.035 % $U_3O_8$ and 0.023 % $U_3O_8$, respectively. The diameter of the hole is 7.8 cm and the outside diameter of the model hole is 1.5 m. The measurements were carried out using four detectors, namely, two Geiger-Mueller counters and two scintillation counters. Experimental results were reduced to the intensity for equal grade and normalized to maximum intensity by a 43 cm layer. The intensity curves thus obtained are given in Fig. 35.

The values of $\kappa$ for each detector are calculated so as to fit the experimental curves by means of least squares. As for the linear absorption coefficient, the value of $\mu=0.2\,\mathrm{cm}^{-1}$ was adopted. This value seems too large compared with the calculated absorption coefficient of water and concrete[10].

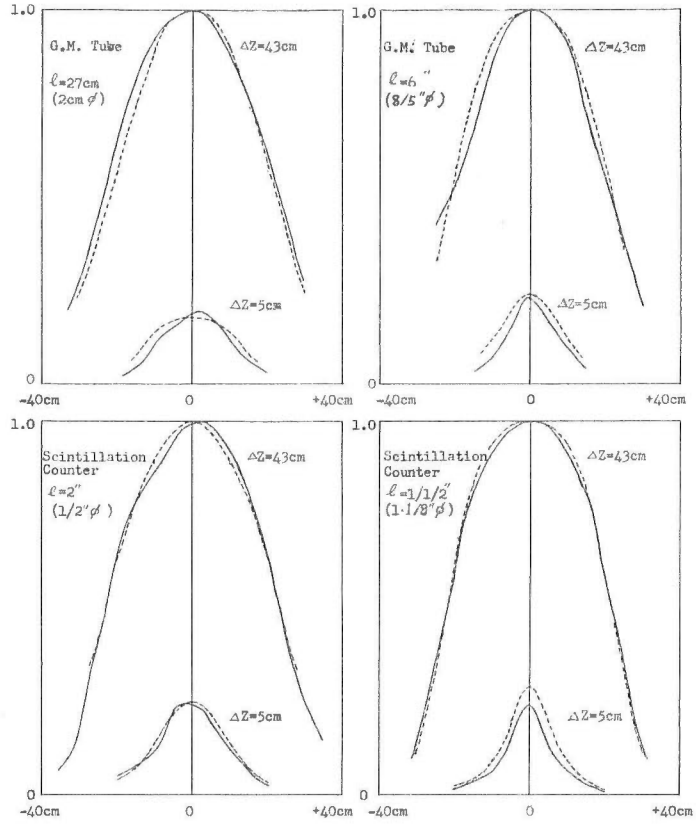


Fig. 35 Experimental intensity distributions measured in a model hole

Table 2

| Detector type | Dimensions of sensitive part | Scattering constant $\kappa$ |
|---|---|---|
| Scintillation counter, NaI(TI) | $2'' \times \frac{1}{2}'' \phi$ | 1.42 |
| Scintillation counter, NaI(TI) | $1\frac{1}{2}'' \times 1\frac{1}{8}'' \phi$ | 0.21 |
| Geiger-Mueller counter | $6'' \times \frac{5}{8}'' \phi$ | 0.00 |
| Geiger-Mueller counter | $27\,\mathrm{cm} \times 2\,\mathrm{cm} \phi$ | 0.00 |

However, if we use values less than $0.2\,\mathrm{cm}^{-1}$, we will have negative values of $\kappa$ in using the Geiger-Mueller counter. The results of the calculation are listed in Table 2; the calculated intensity distributions are compared with the experimental curves as in Fig. 35.

It is clear from the derivation process of expressions for the gamma ray intensity that these values of $\kappa$ contain effects of directional character and finiteness of the diameter of actual detectors. The change in $\kappa$ with detector type does not always depend upon energy response. The difference of $\kappa$ with the two scintillation counters may be explained rather by the differences in actual directional character, since the scintillation counter of 2 inches in sensitive length has a rather remarkable directional character compared with that of the line detector, while the other scintillation counter is nearly non-directional. It may be safely said that the calculated intensity distributions agree with the experimental distributions, considering that assumptions on the detector are simple. Therefore, the Eqs. (38) and (39) will be useful as the approximate formulae for the intensity distribution in a bare drill hole.

In addition, we consider the assumption in Chap. III, that $\mu_1 = 0.2\,\mathrm{cm}^{-1}$ and $\kappa_1 = 1$, is reasonable from the above results.

### V. 4 Estimation of the Ore Reserves in an Ore Bearing Horizontal Bed

In order to estimate the grade and the thickness of the horizontal ore bearing layer, some characteristics of intensity distribution are utilized. For example, the thickness of the layer is obtained from the width at half-maximum intensity, and then the grade is estimated through the ratio of maximum intensity to the intensity of the infinitely thick layer and the relation between the grade and the intensity of the infinitely thick layer. Therefore, a chart, as shown in Fig. 31, is useful for the estimation of the grade and the thickness of the ore bearing layer and is usually prepared by experiments in model holes[2]. If enough artificial radioactive layers are not available to complete the chart, the theoretical expression in Sec. V.2 is made useful by inserting the constants determined by a few artificial layers. The difference between the theoretical and the observed intensity distribution is probably noticed in the case of a large hole diameter, since the detector does not usually pass through the center of drill hole.

If the final aim of the estimation of the grade and the thickness is to obtain the ore reserves in an ore body by drillings extending through the ore body, the mere product of the two quantities is necessary. We now consider the integral $S$ of gamma ray intensity over the depth of the drill

hole, that is, $S=\int_{-\infty}^{+\infty} I^L dZ_0$. Since the variables $Z_0$ and $\xi$ in the integral move along the same $Z$ axis and the interval for $Z_0$ is infinity in each direction, the integral is decomposed to the product of the integral for an elementary layer of thickness of $dZ$ and $\int_{-\Delta Z/2}^{\Delta Z/2} dZ \cdot \int_{-l/2}^{l/2} d\xi = \Delta Z \cdot l$. The integration for an elementary layer is equivalent to the estimation of the intensity from the infinitely thick layer by a point detector. Then, we have

$$S=\int_{-\infty}^{+\infty} I^L dZ_0=(1+\kappa)I_0\sigma\Delta Z\cdot l/\mu. \tag{41}$$

The result is confirmed by many numerical calculations. It will easily be understood that the above relation can be extended to the case where grade is variable with depth.

The counting rate curve is usually affected by the dynamic character of the ratemeter circuit[9]. We denote time constant of the ratemeter by $\tau$, logging speed by $v$, the counting rate curve, which is measured with infinitely slow speed, by $n_0$, and the counting rate curve, which is recorded with logging speed of $v$, by $n$. The expression of $n$ is well known as

$$n=\int_{-\infty}^{Z_0} e^{-\frac{Z_0-Z_0'}{v\tau}} n_0(Z_0')dZ_0'/v\tau,$$

and

$$\int_{-\infty}^{+\infty} n dZ_0=\int_{-\infty}^{+\infty}\int_{-\infty}^{Z_0} e^{-\frac{Z_0-Z_0'}{v\tau}} n_0(Z_0')dZ_0'/v\tau=\int_{-\infty}^{+\infty} n_0(Z_0)dZ_0\,.$$

Therefore, if the area between the counting rate curve and base line in the ratemeter records is $S'$,

$$S'\propto S\propto\sigma\Delta Z\,. \tag{42}$$

This is useful in making the estimation of the product of the grade and the thickness easier.

The error of estimated thickness of ore layer increases with the decrease of thickness itself, as seen in Figs. 31~34. But, the product of the grade and the thickness can be estimated independently of the determination of thickness through the above area method. Moreover, the area method can be applied easily to the case where the grade is variable with the depth. Therefore, the estimation of the ore reserves in the horizontal layer may be performed easily and accurately by radioactivity logging, as long as the suitable value of $I_0$ is used.

## VI. Conclusions

In order to investigate the distribution of gamma ray intensity due to terrestrial radioactivity, the inverse-square exponential law for a point isotropic source combined with a linear build up factor was applied to the calculation of distribution of gamma ray intensity in air and in a drill hole.

The measurement of gamma ray intensity in air from a broad source or an effective half-space was made at various altitudes over a sand area on the coast of the Sea of Japan. The values of scattering constant for air composing build up factor were determined for the detector currently used,

so as to fit the above experimental data assuming several values of absorption coefficient. A reasonable value of scattering constant was obtained in the case of the absorption coefficient of $4.5\times10^{-5}\,cm^{-1}$ for the most penetrating ray from natural radioactive substances. The simple inverse-square exponential law is also applicable to calculations of gamma ray intensity in air by assuming the smaller value of $3.5\times10^{-5}cm^{-1}$ for the absorption coefficient of air. The gamma ray intensities directly over an elementary slab source at various altitudes were calculated by using the constants thus obtained. The results were consistent with the experimental data gained by using a similar detector.

The fundamental formula for a point source was transformed to the expression for an elementary source of infinite thickness. This expression is useful for many problems concerning the intensity distribution in air. The infinitely thick source is represented by the areal distribution on the ground surface. The dimensions of sources equivalent to the broad source were estimated in the case of the circular and infinite slab source, and the results were in agreement with the calculations, which were made by utilizing the different mathematical expression and the analogous experimental data. The intensity distributions over the boundary of two effective broad sources were also calculated.

The intensity distributions from the small thick source and infinite slab source were calculated, as the representatives of infinitely thick sources, in order to supply knowledge on the intensity distributions at various altitudes. The characteristics of distributions, namely, the width at half-maximum intensity and the maximum intensity normalized to the broad source intensity at the altitude of 200 m, were illustrated in the form of charts convenient for the analysis of airborne survey data.

The variations in gradient of the intensity-altitude curve plotted on a semi-log graph were discussed in order to understand the causes of errors in the altitude correction, which usually follows the broad source curve. Excluding clearly exceptional cases, we discussed three possible causes. The most important cause may be the topographic effects, in which the gradients of curve are nearly equal to those of the broad source curve over a definite position of topographic section, but its apparent variations in gradients depend upon the relative directions between the flight line and the topography. The other causes considered are the effect of such surface layer as weathering layer or artificial radioactive substances absorbed in the ground surface, and the indirect effect by airborne radioactive substances. The investigation on the latter two effects has never been done sufficiently because of the lack of the knowledge which has prevented us from directly comparing the effects with airborne survey data.

The intensity distributions in a bare drill hole from a horizontal radioactive layer were calculated by substituting a line detector for an actual one. The substitution is considered to be a proper assumption for the discussion concerning the effects of the detector length and the hole diameter to the response of the detector. The effects expected were theoretically shown in the figures which represent the relationship between the characteristics of intensity distribution and the thickness of the radioactive layer. The figures

show examples of charts estimating the grade and the thickness of an ore bearing layer from a radioactivity log.

The values of constant composing the build up factor were determined for actual detectors by the experimental intensity distribution from artificial ore bearing layers, while the results were affected by the difference in directional character between the theoretical and the actual detector. The theoretical expression is, however, still useful as an approximation for the intensity distribution.

The products of the grade and the thickness of the horizontal ore bearing layer, which are necessary for an estimation of the ore reserves, are obtained by integrating the intensity in the drill hole with respect to its depth, independent of the hole diameter as well as the dynamic character of the ratemeter.

### References


1) Blizard, E. P.: Geometry, Reactor Handbook, Physics prep. by U. S. Atomic Energy Commission, p. 684~693, New York, McGraw-Hill, 1955
2) Broding, R. A. & B. F. Rummerfield: Simultaneous gamma ray and resistance logging as applied to uranium exploration, Geophysics, Vol. 20, No. 4, p. 841~859, 1955
3) Cook, J. C.: An analysis of airborne surveying for surface radioactivity, Geophysics, Vol. 17, No. 3, p. 607~706, 1952
4) Doke, T. et al.: Background radiation from ground surface in Japan (in Japanese), Journal of the Atomic Energy Society of Japan, Vol. 1, No. 1, p. 53~63, 1959
5) Fano, U.: Gamma ray attenuation, Reactor Handbook, Physics, p. 637~666, New York, McGraw-Hill, 1955
6) Godby, E. A. et al.: Aerial prospecting for radioactive materials, National Research Council Laboratory (Canada), Joint Report, MR-17, CRR-495, 1952
7) Kawano, M. et al.: A standard instrument for radon measurement and atmospheric radon content (in Japanese), Proceedings of the Third Symposium on Atomic Energy, Tokyo, Science Council of Japan, 1959
8) Rothè, E.: La methode ionométrique, prospection géophysique, Tome I, p. 315 ~342, Paris, Gauthier-Villers, 1950
9) Sakakura, A. Y.: Scattered gamma rays from thick uranium source, U. S. Geological Survey Bulletin, 1052-A, 1957
10) White, G. R.: X ray attenuation coefficients from 10 KeV to 100 MeV, National Bureau of Standard Report 1003, 1952

## APPENDIX

# Gamma Ray Intensity on the Ground

In the case of the measurement of gamma ray intensity on the ground surface, the detector is usually close to the sources. Generally speaking, the dimension and the shape of the detector should not be negligible, in relation to the replacement of the thick source by the surface distribution as introduced in Sec. IV.1. Calculations of the gamma ray intensity close to the source, therefore, are more complicated practically than intensity in air far away from the source, although the attenuation of gamma rays in air is negligible.

However, in several cases, the estimation of the gamma ray intensity in the neighbourhood of the ground surface can be approximately made by utilizing the modified fundamental formula of the thick source, (15) or (16), for a point detector. The modified formula is reduced to

$$I_T=\frac{I_0\sigma}{4\pi\mu_1}(1+\kappa_1)\frac{\cos\theta}{r_0^2}\rho d\rho\, d\varphi=\frac{I_0\sigma}{4\pi\mu_1}(1+\kappa_1)d(-\cos\theta)d\varphi\,,$$

since $\mu_a$ and $\kappa_a$ are both zero. Then, gamma ray intensity from the broad source is found to be

$$I^B=\frac{I_0\sigma}{2\mu_1}(1+\kappa_1)\,.$$

Gamma ray intensity of the infinite slab source, as shown in Fig. 13, is given by

$$I^I=\frac{I_0\sigma}{2\pi\mu_1}(1+\kappa_1)\Theta\,,$$

where

$$\Theta=\tan^{-1}\left(\frac{Z_0}{x+W/2}\right)-\tan^{-1}\left(\frac{Z_0}{x-W/2}\right).$$

Thus, gamma ray intensity is proportional to the minimum angle between the two planes, which contain the detector and the boundary of the source. The two dimensional topographic effects are easily estimated by using the above result. For example, the gamma ray intensity in the adit of a mine or tunnel, consisting of rock filled homogeneously with a radioactive substance, is

$$I^I=\frac{I_0\sigma}{\mu_1}(1+\kappa_1)=2I^B\,,$$

if the section of arbitrary shape extends uniformly.

## 要　旨

### 地表付近の天然放射能によるガンマ線強度分布について

佐野　浚一

地層中の天然放射能によるガンマ線強度分布に関するいくつかの研究のうちで，A.Y. Sakakura によって発展させられた原理は最も合理的なものと考えられる。しかし，天然放射能の測定に関するかぎり，linear build up factor を用いる方がより適当している。したがって，linear build up factor を伴った点源に対する逆自乗――指数法則を空中および試錐孔中のガンマ線強度分布の計算に適用した。

広い線源すなわち実質的な半無限体による空中のガンマ線強度を種々の高度で日本海沿岸の砂浜の上空で測定した。吸収係数のいくつかの値を仮定して，上記の実験の資料に合うように，現在使用されている検出器について空気に対する build up factor 中の散乱の常数の値を決定した。天然放射性物質からの最も透過力の強いガンマ線に対する吸収係数 $4.5\times10^{-5}\mathrm{cm}^{-1}$ の場合に散乱の常数としてもっともらしい値が得られた。空気の吸収係数として $3.5\times10^{-5}\,\mathrm{cm}^{-1}$ という小さな値を仮定すれば，逆自乗法則もまた空気中のガンマ線強度の計算に適用することができる。小さな板上線源の直上の種々の高度でのガンマ線強度がこのようにして求められた常数を使って計算され，類似の検出器による実験値と一致することが認められた。

点源に対する基本式が無限に厚い微小な線源に対する式に変換されたが，この式は空中の強度分布に関する多くの問題に役立つのである。無限に厚い線源は地表面上の面積的分布によって代表される。円状線源と無限板状線源とについて広い線源と同等になる大きさが計算されたがその結果は異なった数式を使っているが同様な実験資料を使った計算と一致した。2 つの実際的に広い線源の境界上の強度分布も計算された。

無限に厚い線源の代表として，小さい厚い線源および無限板上線源による強度分布が，種々の高度での強度分布の知識を補うために計算された。強度分布の特性，すなわち半値幅と高度 200 m における広い線源の強度に規格化した最大強度とが，空中探査の解析に便利なチャートの形で示された。

高度補正の誤差の原因を調べるために，片対数図上に示される強度――高度曲線の勾配の変化を論じた。高度補正には通常広い線源に対する曲線が用いられる。明らかに例外である場合を除いて 3 つの可能な原因が議論された。最も重要な原因は地形の影響であって，地形断面の一定位置の上空では曲線の勾配は広い線源に対する曲線のそれとほとんど同じであるが，測線と地形の相対的な方向によって勾配の見掛けの変化が起こるのである。他の原因は風化層とか地表面に吸収された人工放射性物質のような表層の影響と空中の放射性物質による間接の影響である。この 2 つの影響に関する研究は空中探査の資料と直接比較できるような知識が足りないので充分行なわれていない。

裸の試錐孔中での水平な放射性層による強度分布が，実際の検出器を線状検出器で表わすことによって計算された。この検出器の置換えは検出器の応答に対する検出器の長さや試錐孔の径の影響を調べるためには適当な仮定であると思われる。直観的に考えられる影響が強度分布の特性と層の厚さとの関係を示す図表によって理論的に示された。この図はまた放射能検層図から鉱石層の品位と厚さとを求めるためのチャートの例でもある。

実際の検出器に対して build up factor 中の常数の値が人工鉱石層による強度分布の実験に

よって決定されたが，結果は理論上の検出器と実際の検出器の指向性の相違の影響を受けている。しかし，理論式は強度分布に対する近似式として有用である。

水平鉱石層の品位と厚さとの積は鉱量計算に必要で，強度を深さについて積分することによって，試錐孔の直径やレートメータの動特性に無関係に求められる。

附録として，地表付近のガンマ線強度が無限に厚い線源に対する基本式によって計算できる場合の簡単な計算例を示した。無限板状線源によるガンマ線強度は検出器が線源を見込む最小の角に比例することが注目される。

**On the Distribution of Gamma Ray Intensity due to Natural Radioactivity near the Earth's Surface** Sano, S.

Shun-ichi Sano

Rept. Geol. Surv. J., No. 188, p. 1~44, 1961
35 illus., 2 tab.

In order to calculate the distribution of gamma ray intensity due to natural radioactivity near the earth's surface, a fundamental formula containing the effect of scattering is proposed and the method for estimating the constants in the formula is presented. The effect of thin surface layers, the topographic effect and the analysis of radioactivity anomaly in the case of air-borne radioactive survey are discussed based on the calculation of intensity distributions. The intensity distributions from horizontal radioactive layers in drill hole are also calculated for the aid of analysis of radioactive logs.

539.166:550.35

The Geological Survey of Japan has published in the past several kinds of reports such as the Memoirs, the Bulletin, and the Report of the Geological Survey.

Hereafter, all reports will be published exclusively in the Reports of the Geological Survey of Japan. The Report will be consecutive to the numbers of the Report of the Imperial Geological Survey of Japan hitherto published. As a general rule, each issue of the Report will have one number, and for convenience's sake, the following classification according to the field of interest will be indicated on each Report.

A. Geology & allied sciences
- a. Geology
- b. Petrology and Mineralogy
- c. Paleontology
- d. Volcanology and Hot Spring
- e. Geophysics
- f. Geochemistry

B. Applied geology
- a. Ore deposits
- b. Coal
- c. Petroleum and Natural gas
- d. Underground water
- e. Agricultural geology Engineering geology
- f. Physical prospecting, Chemical prospecting & Boring

C. Miscellaneous

D. Annual Report of Progress

本所刊行の報文類の種目には従来地質要報・地質調査所報告等があったが，今後はすべて刊行する報文は地質調査所報告に改めることとし，その番号は従来の地質調査所報告を追って附けることにする。そして報告は1報文につき報告1冊を原則とし，その分類の便宜のために次の如くアルファベットによる略号を附けることにする。

A 地質およびその基礎科学に関するもの
- a. 地　質
- b. 岩石・鉱物
- c. 古生物
- d. 火山・温泉
- e. 地球物理
- f. 地球化学

B 応用地質に関するもの
- a. 鉱　床
- b. 石　炭
- c. 石油・天然ガス
- d. 地下水
- e. 農林地質・土木地質
- f. 物理探鉱・化学探鉱および試錐

C その他

D 事業報告

# REPORT, GEOLOGICAL SURVEY OF JAPAN

No. 178

Motojima, K. & Maki, S. : Studies on the brackish water 1. Geochemical studies of Lake Hamana-ko — On the genesis of natural gas accumulation —, 1958 (in Japanese with English abstract)

No. 179

Oana, S. : Studies on the brackish water 2. Determination of the chemical constituents of interstitial water in lake mud and the experiment on the dissolution of organic and inorganic substances from mud of Lake Hamanaka-ko, 1958 (in Japanese with English abstract)

No. 180

Ishiwada, Y. : Studies on the brackish water 3. Recent foraminifera from the brackish Lake Hamana-ko, 1958 (in Japanese with English abstract)

No. 181

Tokunaga, S. : Palynological study on Japanese coal 2. Pollenstratigraphical investigations in the coal fields, middle Hokkaido, 1958 (in Japanese with English abstract)

No. 182

Kaneko, T. : Some aspects of multiple geophone setting and pattern shooting in seismic reflection prospecting, 1959 (in Japanese with English abstract)

No. 183

Motojima, K. : Genetic studies of natural gas accumulations, 1959 (in Japanese with English abstract)

No. 184

Nagumo, S. : On the propagation of transient elastic waves, 1960 (in English)

No. 185

Matsui, H. : On the Toyosato barrier and Ashibetsu basin in the geohistory of the deposition of the upper Ishikari group, Hokkaido, 1960 (in Japanese with English abstract)

No. 186

Motojima, K. : Geochemical study of brine from Yabase oil field, 1960 (in Japanese with English abstract)

No. 187

Tanai, T. & Onoe, T. : A Mio-Pliocene flora from the Ningyo-toge area on the border between Tottori and Okayama prefectures, Japan, 1961 (in English)

# 地質調査所報告

第178号
本島公司・牧　真一：汽水域の研究 I. 浜名湖の地球化学的研究 —— 特に天然ガス鉱床の成因に関連して ——, 1958

第179号
小穴進也：汽水域の研究 II. 浜名湖底質の間隙水化学成分と有機および無機物の溶出機構について, 1958

第180号
石和田靖章：汽水域の研究 III. 浜名湖の現世有孔虫群集 —— 汽水域有孔虫類の研究 ——, 1958

第181号
徳永重元：本邦炭の花粉学的研究 II. 北海道中部諸炭田における花粉層位学的研究, 1958

第182号
金子徹一：地震探鉱における群設置法と多孔爆発法の研究, 1959

第183号
本島公司：天然ガス鉱床の成因的研究, 1959

第184号
Nagumo, S.: On the Propagation of Transient Elastic Waves, 1960

第185号
松井　寛：上部石狩層群の堆積過程における豊里堆と芦別沈降盆地, 1960

第186号
本島公司　他：八橋油田鹹水の地球化学, 1960

第187号
Tanai, T. & Onoe, T.: A Mio-Pliocene Flora from the Ningyo-toge Area on the Border between Tottori and Okayama Prefectures, Japan, 1961

昭和36年2月 5日 印刷
昭和36年2月10日 発行

工業技術院地質調査所

印刷者 笠 井 朝 義
印刷所 笠井出版印刷社



PRINTED BY
KASAI PUBLISHING & PRINTING CO.
(*Pan-Pacific Press*)
MINATO-KU, TOKYO, JAPAN

地質調報
Rept. Geol. Surv. J.
No. 188, 1961